

DETERMINING STRUCTURAL TRANSITIONS THAT OCCUR UPON
GATING A BACTERIAL MECHANOSENSITIVE CHANNEL

APPROVED BY SUPERVISORY COMMITTEE

Paul Blount, Ph.D.

Eric Hansen, Ph.D.

Donald Hilgemann, Ph.D.

David Hendrixson, Ph.D.

DEDICATION

Thank you Lord for the blessings you have given me.

To my parents, without whom I would not have made it this far. Thank you for teaching me to love God and value an education. Thank you for your unconditional love and your continuing inspiration.

**DETERMINING STRUCTURAL TRANSITIONS THAT OCCUR UPON
GATING A BACTERIAL MECHANOSENSITIVE CHANNEL**

by

JESSICA LOUISE BARTLETT

DISSERTATION

Presented to the Faculty of the Graduate School of Biomedical Sciences

The University of Texas Southwestern Medical Center at Dallas

In Partial Fulfillment of the Requirements

For the Degree of

DOCTOR OF PHILOSOPHY

The University of Texas Southwestern Medical Center at Dallas

Dallas, Texas

June, 2006

Copyright

by

Jessica Louise Bartlett, 2006

All Rights Reserved

DETERMINING STRUCTURAL TRANSITIONS THAT OCCUR UPON
GATING A BACTERIAL MECHANOSENSITIVE CHANNEL

Publication No. _____

Jessica Louise Bartlett, Ph.D.

The University of Texas Southwestern Medical Center at Dallas, 2006

Supervising Professor: Paul Blount, Ph.D.

Essentially all bacteria, including pathogens, must be able to rapidly adapt to changing environments, specifically a rapid decrease in osmotic environment which can result in major trauma to the cell. The mechanosensitive channel of large conductance (MscL) is one of a handful of channels that responds to tension in the membrane and acts as a lifesaving mechanism for the cell in instances of osmotic down shock. Solutes are jettisoned before the cell explodes due to internal pressures.

The goal of this project was to further define the mechanism of opening of the MscL channel. I used two approaches to solve this problem. The first utilized the Substituted-Cysteine Accessibility Method (SCAM). Specific amino acids are replaced with a cysteine residue and the ability of that cysteine to react with a substrate is assessed. A cysteine library of the transmembrane domains of *E. coli* MscL was created. I screened the mutants for their ability to react with MTSET before and after shock using whole-cell physiological assays. This *in vivo* SCAM study gave support for a clockwise rotation of TM1 predicted in another model, and defined a number of residues that appear to constitute the pore of the open *E. coli* MscL channel. Furthermore, the precise manner in which the channel activity was modified by the MTSET reagent was then determined by examining a select number of residues using electrophysiology. In this way, the transition from closed to open states could be examined. The data presented confirm many of our previous predictions as well as give new insight into the structural transitions that occur upon gating.

The second approach to define opening utilized functional differences between homologues that have relatively similar sequences. For instance, the *E. coli* and *M. tuberculosis* MscL proteins are similar in sequence. However, they exhibit different sensitivities to pressure both *in vivo* and *in vitro*. Another homologue, found in *S. aureus*, exhibits faster kinetics and a different conductance. The chimeras constructed between *E. coli* and *M. tuberculosis* and

E. coli and *S. aureus* MscLs have given insight into structural domains that can alter channel threshold tension, kinetics and conductance.

TABLE OF CONTENTS

PRIOR PUBLICATIONS.....	IX
FIGURES.....	X
TABLES	X
ABBREVIATIONS	XI
CHAPTER 1 : INTRODUCTION.....	1
BACTERIAL RESPONSES TO HYPEROSMOTIC SHOCK	4
MECHANOSENSITIVE CHANNELS IN BACTERIA	9
STIMULATION OF MECHANOSENSITIVE CHANNELS IN VIVO	11
MSCL STRUCTURE	13
MSCL IN OTHER ORGANISMS.....	14
GATING MECHANISM.....	15
CHAPTER 2 : AN <i>IN VIVO</i> ASSAY IDENTIFIES CHANGES IN RESIDUE ACCESSIBILITY ON MECHANOSENSITIVE CHANNEL GATING	27
INTRODUCTION	27
RESULTS	31
<i>An In Vivo Functional Assay Was Used to Scan the Transmembrane Domains for Residue Positions.....</i>	<i>31</i>
<i>Mutants Targeted by the Primary Screen Fall into Four Major Categories</i>	<i>32</i>
DISCUSSION	33
CHAPTER 3 : MECHANOSENSITIVE CHANNEL GATING TRANSITIONS RESOLVED BY FUNCTIONAL CHANGES UPON PORE MODIFICATION	48
INTRODUCTION	48
RESULTS	52
<i>Utilizing Structural Models and Results from the in vivo SCAM to Functionally Subdivide the Pore Domain.....</i>	<i>52</i>
<i>Modification of Residues Within the Predicted Periplasmic Vestibule Can Effect Dramatic Changes in Open Dwell Times: G26 AND G30.....</i>	<i>53</i>
<i>Modification of Residues Within the Predicted ‘Buried’ Region of the Pore Can Demonstrate Activity-Dependent Changes in Threshold Sensitivity: V23C and I24C</i>	<i>56</i>
DISCUSSION	57
CHAPTER 4 : UNDERSTANDING THE STRUCTURAL DIFFERENCES BETWEEN MSCL ORTHOLOGUES AND HOW THESE DIFFERENCES LEAD TO FUNCTIONAL VARIATIONS	75
INTRODUCTION	75

RESULTS	79
<i>The S1/TM1 Region of MscL Contributes to Stimulus Sensitivity</i>	79
<i>The S. areus MscL Channel Suppresses the Osmotic Lysis Phenotype</i>	81
<i>The S1/TM1 Domains Play a Role Determining the Kinetics of the Channel</i> <i>While the Second Transmembrane Domain Can Influence Conductance</i>	81
DISCUSSION	83
CHAPTER 5 : MATERIALS AND METHODS	96
STRAINS	96
CONSTRUCTION OF CYSTEINE MUTANTS	97
CONSTRUCTION OF CHIMERAS	98
IN VIVO GAIN OF FUNCTION ASSAY	99
IN VIVO FUNCTIONAL ASSAY PERFORMED ON CHIMERA MUTANTS	100
CITRATE-PHOSPHATE DEFINED MEDIA LOGARITHMIC LOF 96-WELL PLATE ..	101
IN VIVO FUNCTIONAL ASSAY PERFORMED ON CYSTEINE MUTANTS.....	103
IN VIVO CYSTEINE ASSAY CITRATE-PHOSPHATE DEFINED MEDIA	105
SPHEROPLAST PREPARATION	106
E. COLI GIANT SPHEROPLAST PREPARATION	109
ELECTROPHYSIOLOGY	110
ANALYSIS	114
CHAPTER 6 : DISCUSSION	121
REFERENCES	134

PRIOR PUBLICATIONS

Bartlett, J. L., G. Levin, and P. Blount (2004). "An *in vivo* assay identifies changes in residue accessibility on mechanosensitive channel gating." Proc Natl Acad Sci USA **101**: 10161-10165.

FIGURES

Figure 1.1 Simple Models of Eukaryotic Mechanosensitive Channels	19
Figure 1.2 Crystal Structures of MscL and MscS.....	21
Figure 1.3 Processes Utilized by Bacteria in Different Environments	22
Figure 1.4 Accumulation and Ejection of Proline	23
Figure 1.5 Five Domains of MscL.....	25
Figure 1.6 Residues Predicted to Reside in the Open Pore.....	26
Figure 2.1 Viability of Cysteine Mutants Challenged by Osmotic Downshock in the Presence of MTSET	43
Figure 2.2 Relative position of reactive TM1 residues.....	45
Figure 2.3 The Location of Reactive Residues Within Current Models for the Closed MscL Channel.....	46
Figure 3.1 Schematic Depictions of the <i>E. coli</i> MscL Emphasizing the Pore Domain and Specific Residues that were Targeted for Substitutions.....	64
Figure 3.2 G26C Locks in an Open Channel Conformation When Modified by MTSET Placed on the Periplasmic Side.....	67
Figure 3.3 G30C Shows Gating-Independent Spontaneous Activity When Modified by MTSET Placed on the Periplasmic, but Not Cytoplasmic Side.....	69
Figure 3.4 V23C Shows Gating-Dependent Spontaneous Activity When Modified by MTSET Placed on the Periplasmic, but Not Cytoplasmic Side	71
Figure 3.5 I24C Shows Gating-Independent Increased Sensitivity When Modified by MTSET on the Periplasmic, but Not Cytoplasmic Side	73
Figure 4.1 Cell Survival Follows the S1-TM1 Domain.....	90
Figure 4.2 Channel Kinetics Follow the S1-TM1.....	92
Figure 4.3 Single Channel Traces Illustrating Channel Kinetics.....	93
Figure 4.4 Channel Conductance Follows TM2	95
Figure 5.1 Multi-round PCR Used to Construct <i>mscL</i> Chimeras	116
Figure 5.2 Visualization of a Patch.....	117

TABLES

Table 2.1 Categorization of Mutants as a Result of the Phenotype Exhibited	41
Table 3.1 Channel Activity in the Presence and Absence of MTSET.....	66
Table 4.1 Quantification of Rescue in <i>in vivo</i> osmotic lysis assay	91
Table 4.2 Patch and <i>in vivo</i> Results for Eco-Sau chimeras.....	94
Table 5.1 Sequences of Primers Used to Make Chimeras	119
Table 5.2 Position of Chimera Junction in Protein and Primers Used.....	120

ABBREVIATIONS

GOF, gain-of-function

TM1, first transmembrane domain

TM2, second transmembrane domain

SCAM, substituted cysteine accessibility method

LOF, loss-of-function

MTSET, [2-(trimethylammonium) ethyl]methanethiosulfonate bromide

Eco, *E. coli*

Tb, *M. tuberculosis*

Sau, *S. aureus*

Chapter 1 : Introduction

Mechanosensation

The ability of cells to respond to mechanical forces is fundamental to survival. Paramecium move away from touch, plants respond to gravity and wind, and humans hear and regulate their blood pressure. A large number of stimuli are perceived through mechanical sensors. Very little is known however, about how these systems work since there is often no binding ligand to easily isolate the channel and they are very often in low abundance in the tissues in which they are found.

In eukaryotic cells, it is thought that the cytoskeleton near the membrane bilayer is often the transmitter of force. For instance, in *Caenorhabditis elegans*, the mechanism of responding to touch has been studied for quite some time using genetic approaches. From very elegant studies, a number of mechanosensitivity (mec) genes have been found (Tavernarakis and Driscoll 1997). Two of these genes, *mec-7* and *mec-12*, encode microtubules. They run the length of the long touch-sensing cells in the worm and if they are disrupted, then the touch sensitivity is lost. It is thought that the microtubules are within a specialized structure. The current model is that the structure is displaced by the touch, the microtubules resist the displacement, and the change is transmitted to the channel

subunits, composed at least partially by the proteins encoded by *mec-4* and *mec-10* (see **Figure 1.1A**). Another system in which force is apparently transmitted through a tether is the vertebrate hair cell (Corey, Garcia-Anoveros et al. 2004). The TRP channel at the tip of one stereocilium is connected to the neighboring stereocilium by filaments called tip links. The deflection of one relative to the other introduces tension in the tip links and causes the channel to open (see **Figure 1.1B**).

The ability to sense mechanical force is not, however, limited to pushing or pulling of channel components; tension within a membrane can be sensed directly. Bacterial mechanosensitive channels, such as the MscL channel and the mechanosensitive channel of small conductance (MscS), are the most studied examples. MscL and MscS have both been cloned, purified, and channel activity monitored in artificial liposomes (see **Figure 1.2**; Sukharev, Blount et al. 1994; Sukharev, Martinac et al. 1994; Chang, Spencer et al. 1998; Levina, Totemeyer et al. 1999; Bass, Strop et al. 2002). They do not need any other molecule to form channel activities. MscL has been examined in a number of lipid environments and showed remarkable versatility to function (Moe and Blount 2005). The stimuli for these channels, in terms of the biophysical changes in the membrane that are detected by the channel, are beginning to be identified. For example, the

shortening of the length of the fatty acid chain seemed to reduce the energy barrier between the closed and open state, but it does not trigger spontaneous openings (Perozo, Cortes et al. 2002; Perozo, Kloda et al. 2002). The force within the pure lipid bilayer, on the other hand, may somehow be detected by the protein; these forces are thought to be extraordinarily large and have been estimated to be on the order of hundreds of dyne cm^{-1} (Lindahl and Edholm 2000). Also, charged amphipaths that intercalate asymmetrically across a membrane that holds a voltage potential can modulate the gating of both MscL and MscS (Martinac, Adler et al. 1990; Perozo, Kloda et al. 2002). Presumably, this is due to the changing of the lateral pressure profile within the membrane. Compounds such as lysophosphatidylcholine, which can be thought of as ‘cone-shaped’ and thus changing the stresses within the membrane as well as the geometry of the patch, triggers the opening of these channels (Perozo, Kloda et al. 2002).

The molecular mechanisms by which bacterial mechanosensitive channels sense and respond to biophysical properties of the membrane may be shared throughout evolution. Eukaryotic channels that respond to tension alone have also been isolated. Similar to bacterial channels, the 2-pore K^+ channels TREK-1 and TRAAK can be activated by force and osmolarity as well as amphipathic chemicals and cone-shaped lipids (Maingret, Patel et al. 2000). They share with

MscL and MscS the common mechanism of mechanosensitive channels whereby they are inhibited by the lanthanide Gd^{3+} , which is thought to work through its interaction with the lipid bilayer (Hamill and McBride 1996; Ermakov, Averbakh et al. 2001).

Regardless of whether these mechanosensitive channels respond to an externally applied force or tension in the membrane, the basic need to sense mechanical stimuli has been preserved. For bacteria, we know that the ability to sense mechanical forces helps the cell respond to environmental hypoosmotic stress (Levina, Totemeyer et al. 1999). In order to understand the role of these channels in osmoregulation, however, it is advantageous to first examine the cells response to hyperosmotic stress.

Bacterial Responses to Hyperosmotic Shock

The bacterial cell is able to thrive in many different types of environments. When grown in a high osmotic environment, the bacterial cell accumulates intracellular osmolytes in order to maintain turgor pressure (see **Figure 1.3**; Dinnbier, Limpinsel et al. 1988). These accumulated osmolytes are referred to as compatible solutes because they can accumulate to high levels within the cytoplasm with little adverse effects. The first molecule to be transported into the

cytoplasm is potassium (Epstein, Wieczorek et al. 1984).. Even at low osmolarities, it is usually the most abundant cation; normally kept at a range of 100-150mM in *E. coli*, this cation can accumulate to approximately 1M concentration (Epstein and Schultz 1965). The hyperosmotic shock triggers the uptake through the three main potassium uptake systems, TrkA, Kup, and Kdp. TrkA and Kup show only about 20% activity in low osmotic conditions because hypoosmotic conditions directly inhibit their activity (Rhoads and Epstein 1978; Laimins, Rhoads et al. 1981). The increased activity of these two systems alone under hyperosmotic conditions is able to restore turgor pressure if the external concentration is above 5mM (Epstein, Wieczorek et al. 1984).

The Kdp operon is expressed only briefly unless potassium transport does not restore turgor. It is a high affinity transport system composed of three structural genes, *kdpABC*, and a two component sensor kinase-response regulator system *kdpDE*. KdpD is in the membrane and appears to sense the potassium levels (Laimins, Rhoads et al. 1981); it has also been postulated to detect biophysical changes in the membrane due to the stress or the relaxation of membrane tension, and to respond to changes in the membrane composition. KdpE is the soluble response regulator that initiates transcription of *kdpABC* (Laimins, Rhoads et al. 1981).

The accumulation of potassium is quickly followed by an accumulation of its counter-ion glutamate through synthesis (Measures 1975). High levels of potassium glutamate are capable of restoring the turgor pressure, but they can also interfere with enzyme function, gene expression, and basic internal protein structure since the amount of free water within the cell is not restored by their accumulation (Csonka 1989).

In order to protect the function of enzymes within the cell, other uptake and synthesis pathways seem to be activated either by the accumulation of potassium glutamate or some other signal. Cells begin to accumulate betaine, proline, and trehalose, if these are available (see **Figure 1.4**; Dinnbier, Limpinsel et al. 1988). Betaine is perhaps the most ubiquitous osmolyte. It can be accumulated to high levels and is not detrimental to cell function (Cairney, Booth et al. 1985). If it is present within the media, ProP and ProU are activated to initiate uptake (Csonka 1988). Cells prefer accumulating osmolytes by transporters rather than synthesizing them, but if betaine is not present, choline can be internalized and converted into betaine. As the amount of betaine increases, the uptake slows, indicating feedback. The amount of betaine in the cell can also affect other osmoprotection systems such as the synthesis of trehalose,

porin synthesis, and DNA supercoiling (Giaever, Snyder et al. 1988). Trehalose has been shown to stabilize membrane structure and its synthesis genes, *OtsAB*, are turned on under hyperosmotic conditions, but the presence of betaine represses the genes indicating that there does seem to be cross-talk in the osmotic-regulatory systems (Giaever, Snyder et al. 1988).

Multiple changes take place within the cell during osmotic shock; one of the most well known is the change in the porin composition (Booth and Louis 1999). In low osmotic environments, OmpF is the main porin present in the outer membrane and in high osmotic environments, OmpC is the major outer membrane pore. Expression of *ompF* and *ompC* is positively regulated through the two component system, EnvZ and OmpR (Booth and Louis 1999). EnvZ may respond to one or more signals within the cell and phosphorylate OmpR. OmpR in turn binds to high and low affinity sites in the promoter for *ompC* and *ompF*. When there is a low amount of phosphorylated OmpR, expression of *ompF* is turned on, but an excess amount of OmpR will bind to a secondary site to suppress expression of *ompF*. This repression can be overcome by addition of betaine (Barron, May et al. 1986). Interestingly, the EnvZ sensor, and its paralogues, some of which are similar to bacterial mechanosensitive channels, appears to be modulated by the biophysical stresses in the membrane as demonstrated by the

apparently direct affects of charged amphipaths that intercalate asymmetrically within the cytoplasmic membrane.

DNA supercoiling is another change within the cell that has been linked to multiple osmoprotectant pathways. When the bacterial cell undergoes a fast transition from a low osmotic environment to a high osmotic environment (hyperosmotic shock), DNA becomes supercoiled (Higgins and Lloyd 1987). This in turn controls expression of the *proU* locus which uptakes betaine. Betaine can reverse the effect as well as gyrases that decrease supercoiling (Higgins and Lloyd 1987). In the opposite manner, TopA increases supercoiling and triggers expression of *proU* (Higgins and Lloyd 1987). Since it is known that DNA supercoiling is determined by the environment and that the first response to hyperosmotic shock is an increase in potassium glutamate, it has been proposed that high concentrations of potassium glutamate may subtly change the structure of the DNA gyrase and/or topoisomerase and thereby affect the changes seen within a cell in this situation.

Mechanosensitive Channels in Bacteria

The ability of bacterial cells to respond to osmotic forces is fundamental to cell survival. As we have seen, when a bacterial cell encounters an increase in osmotic pressure, it accumulates or synthesizes a number of solutes in order to continue growing; in the same manner, if it experiences a drop in osmotic pressure it must release the building internal pressure or lyse (Britten and McClure 1962; Levina, Totemeyer et al. 1999; see **Figure 1.4**). It has been known for many years that *E. coli*, when subjected to a hypoosmotic down shock, jettison a significant amount of their solutes, but maintain macromolecules and begin protein synthesis within minutes (Britten and McClure 1962). After a great deal of searching, mechanosensitive channels were pinpointed as the ‘release valve’ that facilitated this response (Levina, Totemeyer et al. 1999).

An examination of bacterial membranes using the patch clamp technique revealed channels that gated in response to suction applied to the patch (Martinac, Buechner et al. 1987). Three discrete types of channels were isolated in the *E. coli* membrane with increasing conductances that correlated to the pressure required to open them. The channels were labeled the mechanosensitive channel of large

conductance (MscL), small conductance (MscS), and mini conductance (MscM) based upon the size of the pore.

In an attempt to isolate these channel activities, bacterial membranes were fractionated and then assayed for channel activity. After multiple and independent purification steps, a single protein was identified that correlated well with the reconstituted activity. From an N-terminal sequence, the gene for MscL was isolated and the full protein found to be not only necessary, but sufficient, for the MscL channel activity (Sukharev, Blount et al. 1994). The 136 amino acid, inner-membrane protein was predicted to have a helix-loop-helix conformation and to form the channel in a multimeric state (Sukharev, Schroeder et al. 1999). This structural conjecture was confirmed when the *M. tuberculosis* MscL (Tb) was crystallized in a closed or mostly closed conformation to 3.5Å, showing a mainly helical structure with the N and C terminus in the cytoplasm and two transmembrane domains connected by a periplasmic loop (Chang, Spencer et al. 1998; see **Figure 1.2**). Shortly thereafter, the genes coding for MscS activity were isolated (Levina, Totemeyer et al. 1999). *yggB* was found to be responsible for the majority of the mechanosensitive MscS channel activity, while *kefA* encodes a less frequently seen mechanosensitive channel similar in conductance to YggB but regulated by potassium. The channels have since been renamed MscS and MscK (Potassium regulated) for YggB and KefA, respectively. The MscS and

MscK channels share sequence homology; however, MscK is predicted to be substantially larger with a large periplasmic domain and eight additional transmembrane domains prior to the conserved region, which is at the C-terminal of MscK. The *E. coli* MscL and MscS channels have been crystallized, and the MscL channel has five subunits with 136aa per subunit while the MscS channel is a large heptamer structure with 343aa per subunit forming three transmembrane domains and a large cytoplasmic C-terminus (see **Figure 1.2**). MscM, which is only seen infrequently in patch clamping of *E. coli* membranes, has not been isolated nor studied to a great degree. The differences seen in the MscL and MscS structures, coupled with the similar functional response to tension, illustrate that bacterial cells have found more than one structural solution in order to respond to membrane tension.

Stimulation of Mechanosensitive Channels *In Vivo*

The mechanosensitive channels were first postulated to be important for solute release in bacterial populations upon osmotic downshock due to their ability to open in response to membrane tension. Surprisingly, however, the *E. coli* (Eco) MscL null strain showed no phenotype. The first *in vivo* data that linked MscL gating to cellular osmotic responses was when Eco MscL was shown to rescue a normally fragile marine bacterium from osmotic downshock

(Nakamaru, Takahashi et al. 1999). In an attempt to characterize regions of the channel important for gating, mutagenesis was performed; initial studies capitalized on the fact that the channel formed a very large non-selective pore (Blount, Sukharev et al. 1996). Blount *et al.* postulated that mutations which allowed the channel to gate more easily in the cell, could cause the channel to open and destroy the proton motive force in a cell, thereby causing the cell to grow more slowly or cease growth altogether. Random mutagenesis of the entire protein was then undertaken and a number of mutants identified which exhibited this slowed- or no-growth phenotype (referred to as a gain-of-function GOF; Ou, Blount et al. 1998). While the resultant mutants provided insight into the gating of the channel, a specific function for MscL in osmotic sensation was not confirmed until *mscS* was cloned and a mutant constructed lacking both the *mscS* and *mscL* (Levina, Totemeyer et al. 1999). This double mutant was osmotically fragile and showed a decrease in viability upon a hypoosmotic shock which could be rescued by the expression of either *mscL* or *mscS* on a plasmid. These results indicated that the MscS and MscL channels shared a redundant function in an *E. coli* cell, protecting it from lysis due to osmotic downshock.

MscL structure

The MscL channel can be divided into five structural domains: the cytoplasmic N-terminus (S1), the first and second transmembrane domains (TM1 and TM2 respectively), the periplasmic loop connecting the TMs, and the cytoplasmic C-terminus (cytoplasmic bundle; see **Figure 1.5**). The TM1 domains cross and form an aqueous vestibule, open to the periplasm, and narrowing to a constriction point. In the closed or mostly closed *M. tuberculosis* crystal structure, this constriction point is at the analogous Eco MscL residue V23 (Chang, Spencer et al. 1998). Random mutagenesis studies pinpointed the TM1 of the molecule to be important for gating long before the crystal structure was obtained due to the number of GOF mutants isolated along one face of the proposed helices (Ou, Blount et al. 1998). It is thought that these residues in TM1 stabilize the closed conformation of the channel by efficient van der Waals packing, and that changing either the charge or hydrophilicity of a residue in this region can disrupt that packing and effect channel mis-gating. The TM2 packs against the TM1s and interacts with the lipid environment. Mutations isolated in TM2 are often thought to effect gating changes through disruption of lipid headgroup interactions or disruption of interactions with TM1 while gating. The periplasmic loop, which connects TM1 and TM2, has been proposed to act as a ‘spring’ to hold the channel closed (Ajouz, Berrier et al. 2000), and the cytoplasmic N and C termini

have been implicated as a possible second gate (Sukharev, Betanzos et al. 2001) and a filtering mechanism (Anishkin, Gendel et al. 2003), respectively.

MscL in other organisms

Mechanosensitive channels are conserved across a number of species. *mscL*, while not ubiquitous, is maintained in the vast majority of bacterial species as well as at least one archaeon, *Methanosarcina acetovorans*, and one fungus, *Neurospora crassa* (Pivetti, Yen et al. 2003). Over ten of the bacterial homologues have been expressed in *E. coli* membranes and found to encode mechanosensitive channels (Moe, Blount et al. 1998; Folgering, Moe et al. 2005; Jones, Naik et al. 2000; Kloda and Martinac 2001; Nazarenko, Andreev et al. 2003) and/or function to protect an osmotically fragile cell (Moe, Levin et al. 2000), thereby classifying them as orthologues. However, there are functional differences; some gate at a much greater pressure than that of Eco MscL (Tb MscL), while some have shorter open dwell times (*S. aureus* MscL; Moe, Blount et al. 1998). Even though family members are fairly diverse in sequence, most seem to maintain the helix-loop-helix structure and the TM1 is the most well conserved portion in both length and sequence (Pivetti, Yen et al. 2003), consistent with this domain forming the pore of the channel.

Gating Mechanism

The mechanism by which MscL and MscS open a channel pore in response to tension in the membrane is of great interest because the lessons learned from these 'simple' channels can be utilized to not only describe bacterial responses to environmental osmolarity, but might also be applied to how more complex stretch-activated channels sense tension and respond. The stimulus that the MscL channel senses has often been postulated to be tension alone since activity could be seen when the channel was reconstitution into a lipid bilayer (Sukharev, Blount et al. 1994); this has since been confirmed through specific examination of the pressure profile in relation to the geometry of the patch (Moe and Blount 2002). The mechanism of how the channel senses that tension is still being investigated, but basic components that have been implicated are the physical state or fluidity of the membrane, intrinsic curvature, and hydrophobic mismatch (Perozo, Kloda et al. 2002; Gullingsrud, Schulten et al. 2003).

The fluidity of a membrane, or the basic ability of lipids to freely diffuse, and its effect on mechanosensitive channels is a complex issue. The fluidity is determined not only by temperature but also by the lipid composition. Interestingly, *E. coli* grown at lower temperatures will change the composition of their membrane in order to maintain a certain fluidity. Observations by Blount and colleagues have indicated that cooling of the membrane *in vitro* may increase

the open probability of MscL (personal communication). This could indicate that a more dense packing order increases MscL gating. Pure composition of the membrane has also been shown to effect channel activity (Moe and Blount 2005). Amphipaths are thought to decrease the packing order of the membrane and their addition to the lipid bilayer has been shown to shift the opening of MscL to lower pressures (Martinac, Adler et al. 1990). Gadolinium, however, which interacts with the headgroups of the lipids and changes the mechanical properties of the bilayer (Ermakov, Averbakh et al. 2001), inhibits gating of mechanosensitive channels from both eukaryotic and prokaryotic organisms (Berrier, Coulombe et al. 1992). The fluidity of the membrane is a very complex component and while it is definitely a factor, it is not thought to trigger conformational changes in channels, just to influence the rate at which changes take place (Lee 1998).

The ability of membrane curvature and bilayer thickness to activate channel gating has also been studied. Unfortunately, the lipid shapes that change curvature also change membrane thickness making the interpretation of curvature contribution difficult. The affect of bilayer thickness alone has been examined, however. The bilayer immediately adjacent to the protein will tend to match the length of the protein's hydrophobic exterior. Since any change in the area of the membrane (such as a volume expansion of the cell) should be accompanied by a proportional change in membrane thickness, the match between the hydrophobic

core of the channel and the lipid bilayer may be important in determining the stability of different channel conformations. There would be an energetic cost to exposing hydrophobic residues or burying polar residues. Indeed, the affect of membrane thickness has been observed by reconstituting the MscL channel into defined lipids with different chain lengths. The shorter bilayers seemed to lower the threshold sensitivity, but based on EPR spectroscopy did not induce structural changes (Perozo, Kloda et al. 2002). Therefore, mismatch alone is not the primary triggering element. The incorporation of lysophosphocholine, however, produced spontaneous openings (Perozo, Kloda et al. 2002). All of these data taken together indicate that the lateral pressure profile may be the main parameter that is conferring the ability to gate.

This transduction of energy from the lipid to the channel may be exerted on the entire channel or just specific locations within the channel. Mutagenic studies found a clustering of LOF mutants near the region that should interact with the lipid headgroups (Maurer and Dougherty 2003). Furthermore, asparagine scanning and tryptophan mutagenesis identified bands of hydrophobic residues at the periplasmic and cytoplasmic sides, respectively, that may constitute tension sensors (Maurer and Dougherty 2003; Powl, Wright et al. 2005).

Since the crystallization of *M. tuberculosis* MscL, two basic models of gating have been proposed for the channel. Both involve the tilting of TM1 and TM2 within the stretched and thinning membrane (Sukharev, Durell et al. 2001; Betanzos, Chiang et al. 2002; Perozo, Cortes et al. 2002), allowing TM1 to form the pore of the open channel. However, the two models differ in the specific residues likely to line the open pore (**Figure 1.6**). The Perozo-Martinac (PM) model (Perozo, Kloda et al. 2001) suggests a clockwise rotation of TM1 while the Sukharev-Guy (SG) model (Sukharev, Betanzos et al. 2001) suggests a counter-clockwise rotation. Also, the SG model proposes a pre-conducting expansion of TM1 with the S1 helices forming a second gate (Sukharev, Betanzos et al. 2001), even though most functional data and energetic parameters can be interpreted to support only a single gate in MscL (Hamill and Martinac 2001).

The movements within the channel during gating, and the potential role of domains in the functional differences observed between some orthologues, have been further examined in this study. Residues within the channel pore have been identified by using a modified *in vivo* substituted cysteine accessibility method (SCAM) and functional modifications in the pore have been examined using the patch clamp technique. This has allowed us to gain insight into the gating of a bacterial mechanosensitive channel.

Figure 1.1 Simple Models of Eukaryotic Mechanosensitive Channels

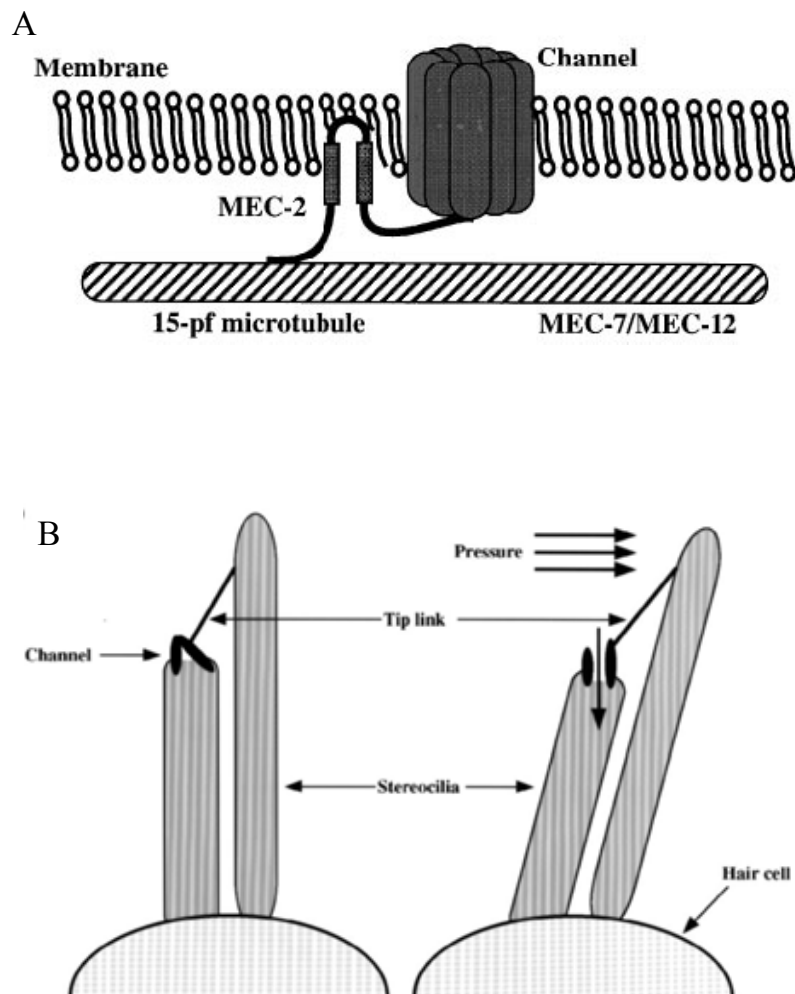


Figure 1.1 (A) A pictorial example of how the *C. elegans* MEC channel may be opened through a tether. In touch-sensitive neurons, the Mec-2 protein may be interacting with the internal microtubules and attached to the channel. The small portion intercalated into the membrane may act as a fulcrum to transmit microtubule deflection. (B) A pictorial example of how mechanosensitive channels of the hair cell may be opened. Channels located at the tip of the stereocilia may be pulled open by the tip link when the stereocilia are deflected. Figure modified from (Tavernarakis and Driscoll 1997).

Figure 1.2 Crystal Structures of MscL and MscS

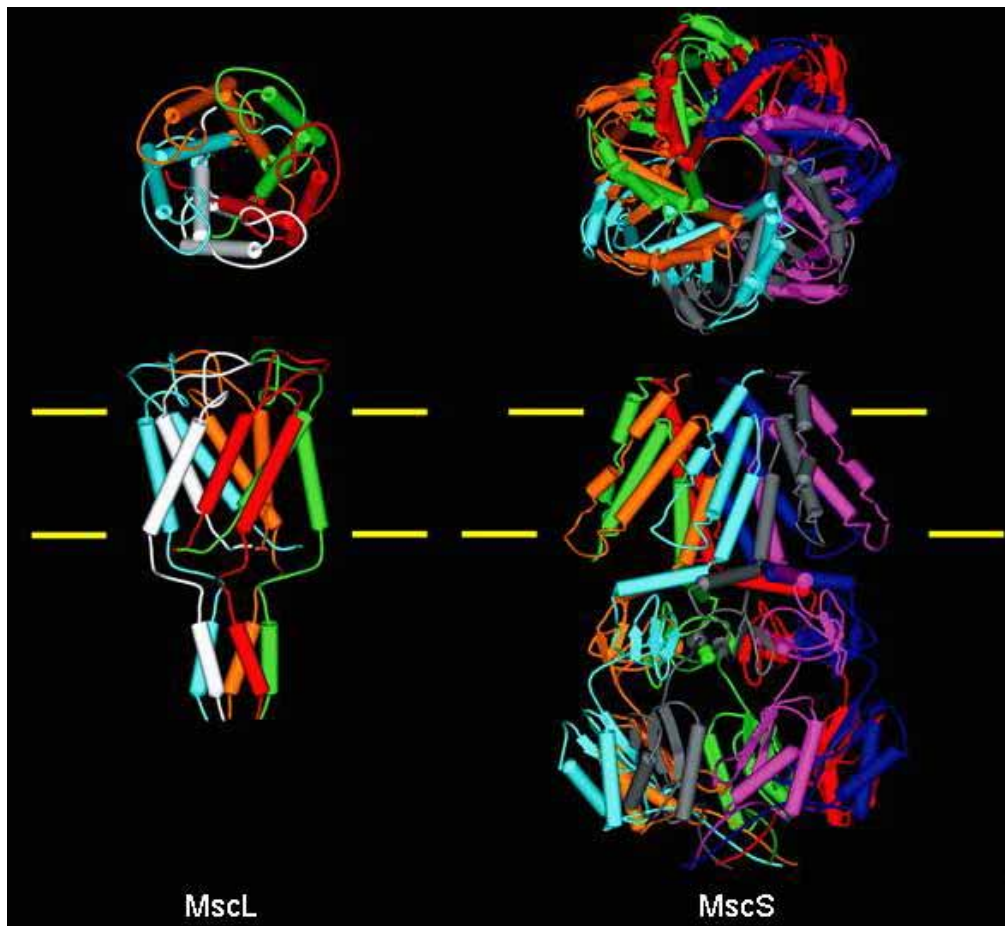


Figure 1.2 The crystal structures of MscL and MscS. On the left is a closed structure of MscL the top view is seen from the periplasm looking down. The bottom view is looking across the membrane with the yellow lines representing the membrane. On the right is the crystal structure of MscS in an open conformation. Separate subunits are colored differently. Modified from (Blount 2003)

Figure 1.3 Processes Utilized by Bacteria in Different Environments

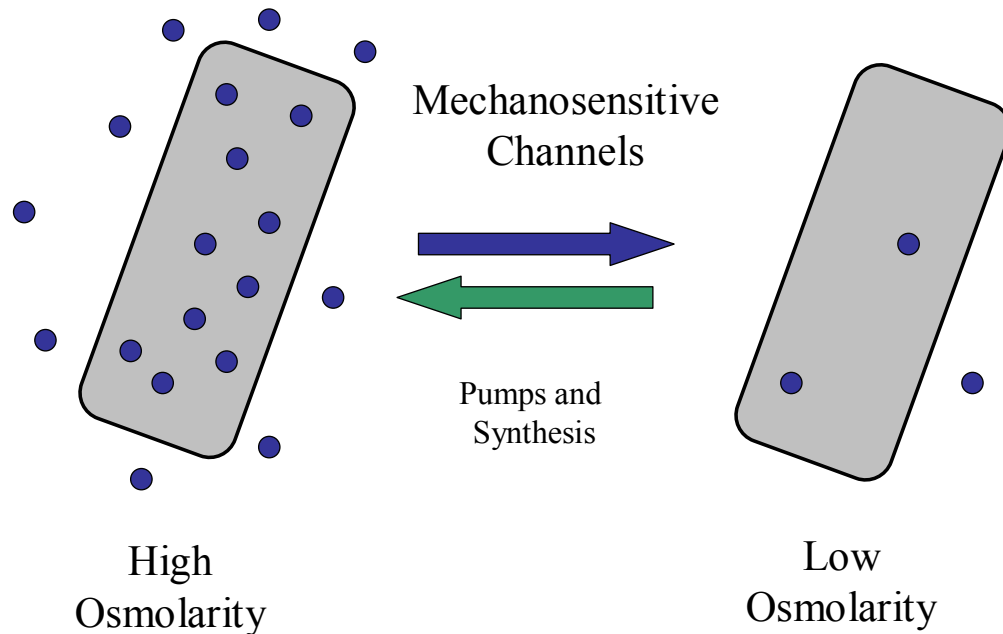


Figure 1.3 A pictorial example of how the bacterial cell maintains a homeostatic relationship with the environment concerning osmolarity. Blue dots represent solutes. In a high osmotic environment, the cell must accumulate a large amount of internal solutes to maintain turgor pressure, while relatively few solutes are required in a low osmotic environment. Rapid transitions between the environments put the cell at risk for plasmolysis (going from low to high osmolarity) or lysis (going from high to low osmolarity). The cells take up and/or synthesis compatible solutes and open mechanosensitive channels, respectively, to regain homeostasis with the environment.

Figure 1.4 Accumulation and Ejection of Proline

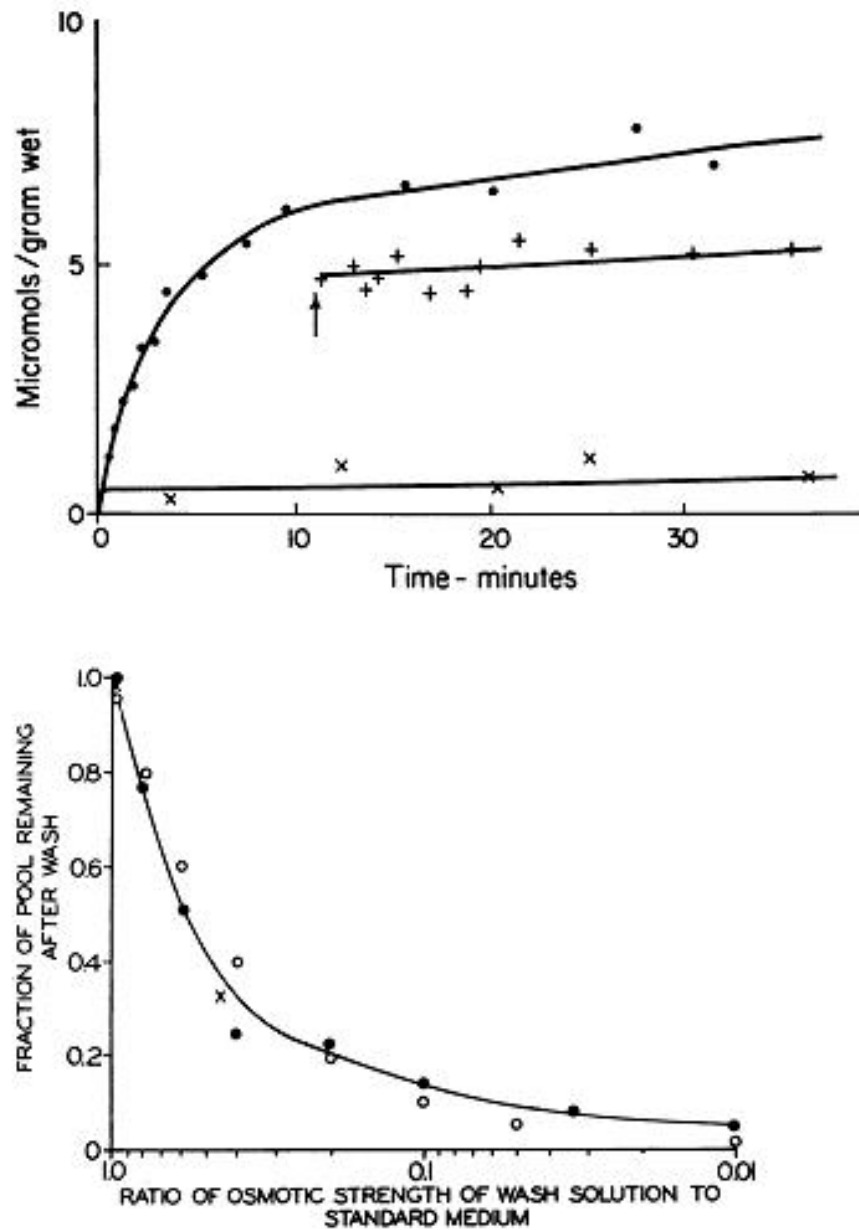


Figure 1.4 (A) The ability of *E. coli* to maintain internal proline concentrations is not dependent on proline being maintained in the medium. The total proline incorporation into proteins within the cell is represented by (x). The dark circles represent the amount of radioactive proline present in the cell. The crosses represent the amount of proline within the cell after external proline was diluted away. (B) Osmotic downshock causes the loss of internal proline pools. Cells were washed with solutions of various osmolarities compared to the standard medium. The dark circles represent cells that were washed with various dilutions of the standard growth medium, the open circles represent cells that were washed with NaCl solutions, and those washed with glucose solutions are indicated by (x). Modified from (Britten and McClure 1962).

Figure 1.5 Five Domains of MscL

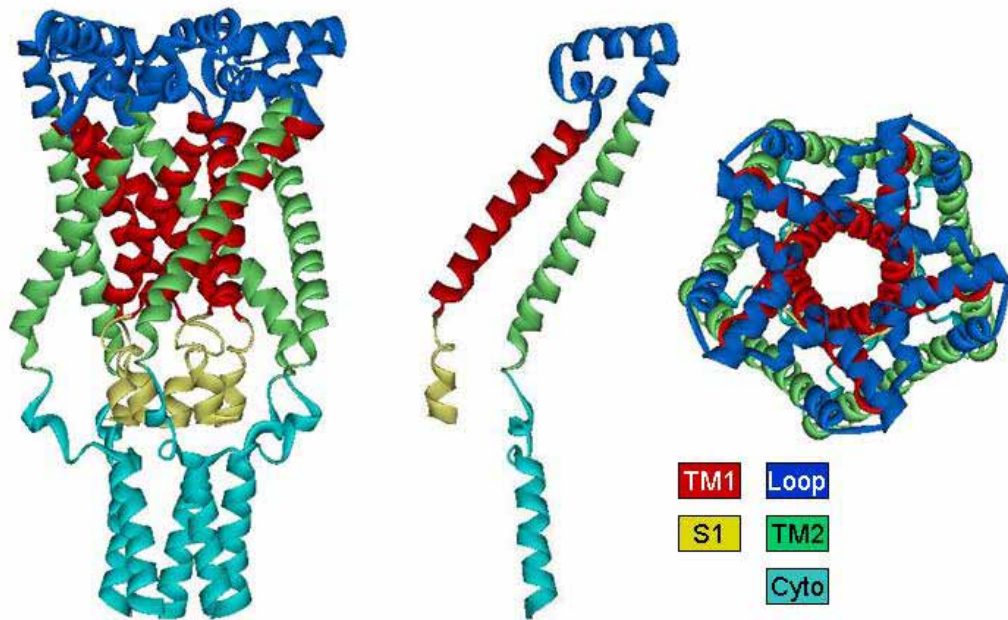


Figure 1.5 The model of *E. coli* MscL; from left to right, the full channel seen across the membrane, a single subunit, and a periplasmic view of the channel. The model is colored based on the five simple structural domains. The legend indicates the name of each domain.

Figure 1.6 Residues Predicted to Reside in the Open Pore

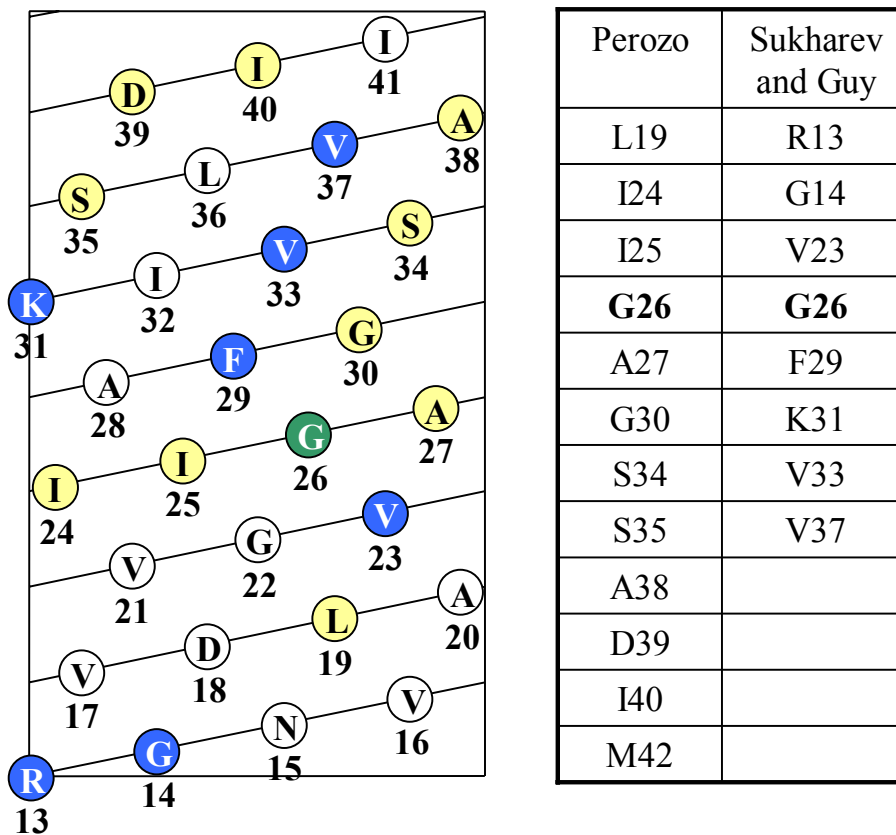


Figure 1.6 An idealized helical net of TM1 from *E. coli* MscL is shown. The residues predicted to be exposed by the Perozo model are colored in yellow (Perozo, Cortes, et al. 2002). The residues predicted to be exposed by the Sukharev-Guy model are colored in blue (Sukharev, Durell, et al. 2001). The only residue that is the same in both models, G26, is colored in green and bolded in the table. The table lists the specific residues in TM1 that are exposed from each model.

Chapter 2 An *in vivo* assay identifies changes in residue accessibility on mechanosensitive channel gating

Introduction

The ability to detect mechanical force is crucial for essentially all life. One paradigm, which has been well studied at the molecular and structural levels, is the ability of microbes to detect membrane stretch invoked by the osmotic environment. *Escherichia coli* contains two mechanosensitive channels that have been shown to be involved in osmotic regulation, MscL and MscS (Levina, Totemeyer et al. 1999). Homologues of these molecules are found in virtually all microbes, including the Archea (Pivetti, Yen et al. 2003). The genes appear to encode proteins that serve a redundant function in osmotic adaptation because deletion of both *mscS* and *mscL* is required to observe a phenotype (Levina, Totemeyer et al. 1999). The resulting double-null strain is osmotically fragile, showing reduced viability on acute hypotonic shock (osmotic downshock).

To date, MscL is the best-studied mechanosensitive channel. Many mutations that effect a gain-of-function (GOF) phenotype, in which the cells show slowed growth or decreased viability, have been isolated and studied (Ou, Blount

et al. 1998; Yoshimura, Batiza et al. 1999; Maurer and Dougherty 2003; Levin and Blount 2004). The pivotal point came when a crystal structure of an orthologous channel from *Mycobacterium tuberculosis* was resolved to 3.5 Å (Chang, Spencer et al. 1998). The channel was found to be a homopentamer. However, the study could not determine whether the solved structure reflects a closed or "nearly closed" state of the channel (the channel constricted to a 4-Å-diameter pore), nor could it accurately predict the structural changes that occur on channel gating. What was clear from the crystal structure was that the first transmembrane domain (TM1) lines the lumen and that to obtain the predicted open-pore size of >30 Å in diameter (Cruickshank, Minchin et al. 1997), large structural changes must occur. Subsequent studies have predicted features of the channels' open structure; one suggested model is based on modeling, crosslinking, and disulfide-trapping experiments (Sukharev, Durell et al. 2001; Betanzos, Chiang et al. 2002), and the other is based on EPR results (Perozo, Cortes et al. 2002). Although agreement exists on general aspects of gating, such as tilting of the transmembrane domains, several fundamental differences exist, including the identity of specific residues likely to line the open pore.

One approach that has been often used for identifying residues within a channel pore is the substituted cysteine accessibility method (SCAM; Akabas and Karlin 1999). In the SCAM, cysteine substitutions are generated within the

protein and sulfhydryl reagents are allowed to react on gating. Hydrophilic, often charged, reagents are typically used to assure that only residues that are accessible to the aqueous environment are modified. If the residue is buried within the closed channel but exposed on gating, then the reagent will react with the cysteine only on channel opening. For channels with small pore sizes, a decrease in conductance is often observed on this modification.

Recently, Batiza et al. (Batiza, Kuo et al. 2002), studying *E. coli* MscL, adapted the SCAM to test for accessibility in vivo. This group exploited previous observations demonstrating that hydrophilic or charged substitutions within TM1 often lead to decreased viability (Ou, Blount et al. 1998; Yoshimura, Batiza et al. 1999). This appears to be due to channel misgating because patch clamp analysis demonstrated that the channels gate at lower than-normal membrane tensions. In addition, reaction of charged sulfhydryl reagents with a cysteine mutant, G22C, demonstrated that these changes could be effected *in situ*, as assayed by patch clamp (Yoshimura, Batiza et al. 2001). Batiza et al. (Batiza, Kuo et al. 2002) studied the accessibility of a mutant with a single substitution, L19C, and found a decreased viability on treatment of the charged sulfhydryl reagent, [2-(trimethylammonium) ethyl]methanethiosulfonate bromide (MTSET), with intact cells. This decrease in viability was observed only when the channel was gated by

an acute osmotic downshock, suggesting that the residue was only exposed on gating.

We recently generated a mutant library in which every amino acid in the transmembrane domains had been sequentially replaced with cysteine. Because wild-type *E. coli* MscL contains no cysteines, each substituted cysteine is unique within the subunit. Every mutant in the library was assayed for its ability to confer phenotypic changes, and many were characterized electrophysiologically (Levin and Blount 2004). Although not as severe as reported (Ou, Blount et al. 1998; Yoshimura, Batiza et al. 1999; Maurer and Dougherty 2003; Levin and Blount 2004), GOF-affecting cysteine substitutions were noted in the middle of TM1, near the proposed channel constriction point and toward the periplasmic and cytoplasmic regions of the second transmembrane domain (TM2). Here, we use this characterized library for a modified *in vivo* SCAM. The ability to drastically decrease viability on residue modification allows us the unique ability to resolve aspects of the structure of MscL in different conformational states while it resides in a living cell. Although our results are consistent with the overall predictions of the crystal structure, they suggest modifications needed to define the fully closed state of the channel. Our results also provide strong support for one of the contested models for structural changes that occur during channel gating.

Results

An *In Vivo* Functional Assay Was Used to Scan the Transmembrane

Domains for Residue Positions

The *in vivo* SCAM was used to identify the amino acids of MscL that are exposed to the aqueous environment on channel gating. We used a transmembrane domain cysteine library to assay all residues within TM1 and TM2 (Levina, Totemeyer et al. 1999). The mutated proteins were expressed in an *mscL*, *mscS* double-null strain (MJF455). In the primary screen, the library was exposed simultaneously to both the positively charged sulfhydryl reagent MTSET and acute osmotic down-shock. The treated cells were then plated and viability scored. As seen in **Figure 2.1**, several of the cysteine mutants demonstrated a significant decrease in viability on treatment. Mutants exhibiting <60% viability were targeted for further study.

All mutants were initially tested after 1 h of β -D-thiogalactoside induction. However, consistent with a previous study (Levin and Blount 2004), at induced expression levels V23C conferred a GOF phenotype that led to a viability too low to measure. Therefore, V23C was assayed in the absence of induced expression. Previous studies had demonstrated that without induction the vector allows the expression of two to six channels per cell (Blount, Sukharev et al. 1999). As

shown in **Figure 2.1**, even at such low expression levels, the viability ratio of treated to untreated V23A-containing cells was quite low for this mutant, supporting it as a candidate for further study.

Mutants Targeted by the Primary Screen Fall into Four Major Categories

At this point we sought to exclude mutants that form a nonfunctional channel, or are loss-of-function (LOF), and thus are not suitable reporters of residue accessibility on gating. Toward this end, we assayed all the mutants indicated by the initial screen for their viability subsequent to the osmotic downshock in the absence of MTSET treatment. The double-null MJF455 strain used in this study, lacking both *mscS* and *mscL*, normally shows decreased viability on acute osmotic downshock. Expression of a functional MscL channel rescues this osmotic lysis phenotype, even at uninduced expression levels [see wild type (**Figure 2.1** and V23C (**Table 2.1**)), which we know to be only a few channels per cell (Blount, Sukharev et al. 1999). We assayed all of the mutants for their viability subsequent to the osmotic downshock in the absence of MTSET treatment. As seen in **Table 2.1, group I**, seven of the 19 candidates identified in the primary screen were determined to be LOF by their inability to rescue this osmotic-lysis phenotype.

The remaining 12 candidates identified in the primary screen showed decreased viability only in the presence of MTSET. To determine whether MTSET was reacting with the channel when in the closed state, we tested viability in the absence of osmotic downshock. Four candidates demonstrated decreased viability on MTSET treatment alone (**Table 2.1, group II**). In contrast, seven of the candidates showed decreased viability that depended on both MTSET and osmotic downshock (**Table 2.1, groups IIIa and IIIb**). Four of these demonstrated some decrease in viability when treated with MTSET alone (**group IIIa**). R13C was assigned to a fourth category, **group IV**, because it showed the interesting property that MTSET actually increased viability on osmotic downshock.

Discussion

The modified SCAM used here allowed us to identify MscL transmembrane residues exposed in different conformational states while the channel is within its native environment of a living cell. Sulfhydryl reagents, including methanethiosulfonate compounds, have been used in the past to probe the pore of several other channels (Akabas and Karlin 1999). However, the pore of the MscL channel is much larger than those other channels and is estimated to be 30 Å (Cruickshank, Minchin et al. 1997). Therefore, it seems unlikely that

MTSET would block the passage of ions, as is observed for other channels. Instead, the assay depends on the assumption that the addition of a large hydrophilic group onto the residue will cause the channel to gate more easily. Precedent exists: previous studies found that hydrophilic substitutions within the TM1 domain, which lines the pore (Chang, Spencer et al. 1998), leads to channels that gate at lower membrane tension, thus resulting in a GOF phenotype (Ou, Blount et al. 1998; Yoshimura, Batiza et al. 1999; Maurer and Dougherty 2003). These substitutions appear to result in channels that more easily go through transitions between closed and open states (Blount and Moe 1999; Yoshimura, Batiza et al. 1999). The assumption appears to be valid given the finding that at least one substituted residue per -helical turn of the pore forming region of TM1 was found to lead to MTSET-dependent decreases in viability (**Figure 2.2**).

Although the primary screen used here does not distinguish between mutated residues that become exposed on channel gating and those conferring constitutive LOF phenotypes, it is a simple matter to distinguish among these categories on subsequent analysis. In the previous study in which MTSET was used to identify a residue exposed on gating, the authors used several *mscL*-null host strains (Batiza, Kuo et al. 2002). Here, we have specifically used an *mscL* and *mscS* double-null strain, MJF455 (Levina, Totemeyer et al. 1999). This use has the advantage of avoiding false-negative results; if a channel is functionally

compromised and is significantly less sensitive than normal, then the MscS channel cannot shunt the turgor forces induced by the osmotic downshock. However, because the double-null strain is osmotically fragile, this approach will also identify nonfunctional or LOF mutants. A decreased viability could also be due to MTSET binding in the closed state and lead to a nonfunctional channel that induces lysis on osmotic shock. However, group IIIa shows a phenotype independent of shock, and mutations in group IIIb gave consistent results when performed in PB104 (Blount, Sukharev et al. 1996; Ou, Blount et al. 1998), a MscS-containing strain (Batiza, Kuo et al. 2002, and data not shown). The cysteine library used here has been characterized previously; although the vast majority of mutants were shown to be functional, a few conferred LOF phenotypes due to misfunctioning channels, as opposed to heterologous or decreased expression levels (Levin and Blount 2004). Although the osmotic downshock procedure was different between the original study and the present one, a strong agreement exists between the two; most of the mutants we identify as LOF here (group I) are consistent with the previous study. A few mutants, specifically Q80C, F85C, and A89C, were categorized as LOF in the previous study but were not recognized here, presumably because of differing experimental conditions; none of these mutants were shown to react with MTSET. In addition, we categorize G76C and I92C as LOF; these mutants were not assayed in the previous study because of their GOF phenotype. These mutants may not truly be

nonfunctional, but the compromised viability in the LOF assay may in fact be due to the combined stresses of the GOF phenotype (misgating or leaking channels) combined with osmotic downshock.

We found that R13C appears to be sensitive to osmotic downshock alone but is saved by the addition of MTSET (**Table 2.1, group IV**). The R13C substitution has been shown to confer a GOF phenotype (Levin and Blount 2004). As with G76C and I92C (discussed above), the LOF phenotype may in fact be due to the combined stresses of the GOF phenotype and osmotic downshock. A likely interpretation is that introduction of the positively charged MTSET restores channel function, and thus viability, because the positive charge at this position is reestablished.

The results presented here give us an image of the vestibule portion of the pore. Several residues reacted with MTSET independent of osmotic downshock and elicited a loss of viability phenotype (group II). These residues reside within the more periplasmic portion of TM1 (**Figure 2.2**). Although we cannot completely rule out the possibility that the cysteine substitution influences the structure for a given mutated MscL, it is impressive that when modeled onto the crystal structure of the *M. tuberculosis* MscL channel (Chang, Spencer et al. 1998), the residues appear to line one face of the helix (**Figure 2.3**). Note,

however, that they do not directly face the lumen but are rotated several degrees clockwise as viewed from the periplasm. Although when the MscL channel was originally crystallized, the authors noted that it appeared to be in a closed or "nearly closed" state (Chang, Spencer et al. 1998), it has more recently become dogma that the crystal structure reflects the closed conformation. Recently, a proposal was made that the current structural models, including the crystal structure, do indeed reflect a "nearly closed" state and that a slight counterclockwise rotation of TM1 is necessary to achieve the native closed state (Levin and Blount 2004). The evidence underlying this proposal was the formation of a disulfide bridge for a single cysteine mutant, G26C. Here, we find four residues that appear to be exposed in the closed state that support this hypothesis (**Figure 2.3**). In sum, the findings are consistent with the clockwise direction of rotation for TM1 during gating (counterclockwise for closure) suggested by data obtained from site-directed spin-labeling and EPR spectroscopy (Perozo, Cortes et al. 2002) but not consistent with the countermodel for gating that proposes a slight rotation in the opposite direction (Sukharev, Durell et al. 2001; Betanzos, Chiang et al. 2002).

Several residues showed changes in MTSET accessibility on osmotic shock. G30C showed an apparent decrease in accessibility on shock (note the difference between MTSET + shock vs. MTSET-alone values), suggesting that

the residue is buried on channel opening. Some mutants required both exposure to MTSET and osmotic downshock for the largest decrease in viability (groups IIIa and IIIb), suggesting that these residues are inaccessible in the closed state but become exposed on gating (**Figure 2.2**). In a previous study, V23C and V37C were identified as conferring a strong GOF phenotype when expressed (Levin and Blount 2004). Hence, the small but measurable accessibility of MTSET to these residues in the absence of osmotic downshock may simply be that the reagent can react with channels that are misgating *in vivo*. Similarly, G26 confers a GOF phenotype and may actually require gating for reactivity. Hence, for members of group IIIa, and even for selected members of group II, we may be underestimating the requirement of channel gating for MTSET reactivity.

A careful examination of residues categorized within groups IIIa and IIIb can help to predict a profile for the open-pore and transition-state structures. Consistent with the hypothesis that little if any of TM2 lines the pore (Sukharev, Durell et al. 2001), we found only TM1 mutants within these groups. Two of these TM1 residues reside close to the periplasm, V37 and M42. Presumably these residues are obscured by the periplasmic loop structure and are revealed on gating. Exposure of more cytoplasmic residues may occur in either of two conditions: either the residue is buried within the protein and exposed as the channel opens, or the residue resides within the cytoplasmic compartment and

becomes accessible when the channel allows the reagent to flow into the cell. L19C, which is the most cytoplasmic residue identified within these categories, has previously been shown by patch clamp to not be accessible to MTSET when it was placed within the bath of an excised patch (i.e., the cytoplasmic side). A similar electrophysiological study with G22C found that MTSET has some access to this residue when applied to the periplasmic (pipette) but not the cytoplasmic (bath) side of a patch (Yoshimura, Batiza et al. 2001). Because V23 and I24 are more periplasmic in location, it seems likely that they would also not be accessible from the cytoplasmic side (**Figure 2.2**). This interpretation is consistent with the crystal structure, which suggests these residues are buried within a tightly packed bundle of TM1 helices surrounded by TM2s.

Perhaps the most significant finding is that I24 is exposed on gating. This residue is tangential to the constriction point of the closed pore. The crystal structure suggests that the constriction point of the closed pore is V23 (V21 in *M. tuberculosis*; Chang, Spencer et al. 1998); but, as discussed above, the disulfide bridging of G26C suggested that this residue may be the constriction point in the fully closed state (Levin and Blount 2004). The latter interpretation is more consistent with the data presented here (**Figures 2.2 and 2.3**). Regardless, exposure of I24 to the pore lumen would require a significant clockwise rotation of TM1. Here again, the data support the clockwise rotation of TM1 on channel

gating as proposed (Perozo, Cortes et al. 2002). In the alternative model proposed by Sukharev et al. (Sukharev, Durell et al. 2001), F29, not I24, is predicted to line the open pore. Because F29 is on the opposite face of the helix as I24 (**Figure 2.2**), the data presented here strongly suggest that the Sukharev *et al.* model is incorrect in its predictions of residues lining the open pore. Hence, by using an *in vivo* SCAM, we have been able to identify residues lining the lumen of the pore in different conformational states of the molecule, support modifications of the closed-state models of the channel, and provide support for a clockwise rotation of the pore-forming first transmembrane domain on gating.

Table 2.1 Categorization of Mutants as a Result of the Phenotype Exhibited

	Osmotic Shock	MTSET	MTSET + Osmotic Shock
Empty Vector	4.6 ± 0.2	122 ± 1	3.3 ± 0.1
<i>E. coli</i> MscL	93 ± 1	96 ± 1	85 ± 1
Group I			
G14C	16 ± 1	122 ± 3	24 ± 2
D18C	26 ± 9	113 ± 10	18 ± 6
K31C	29 ± 3	116 ± 9	35 ± 1
L36C	33 ± 4	87 ± 4	11 ± 1
G76C	40 ± 2	96 ± 8	25 ± 5
I92C	56 ± 4	111 ± 5	41 ± 2
F93C	47 ± 2	107 ± 4	49 ± 3
Group II			
G26C	13 ± 2	≤0.2	≤0.2
G30C	79 ± 4	≤0.2	25 ± 3
S34C	89 ± 15	≤0.2	≤0.2
A38C	85 ± 3	61 ± 4	55 ± 1
Group III_a			
G22C	80 ± 2	48 ± 6	0.60 ± 0.08
V23C*	83 ± 4	45 ± 7	12 ± 1
A27C	94 ± 6	54 ± 2	43 ± 2
V37C	95 ± 3	56 ± 3	28 ± 4
Group III_b			
L19C	115 ± 19	129 ± 13	14 ± 6
I24C	87 ± 2	92 ± 2	22 ± 4
M42C	78 ± 8	64 ± 9	3.3 ± 0.6
Group IV			
R13C	6 ± 3	107 ± 3	57 ± 10

Table 2.1 Shown is the percent survival \pm SEM under the different conditions assayed. All experiments were performed in duplicate with three or more independent experiments. The first column indicates the ability of the cells to survive osmotic downshock alone, the second indicates their ability to survive MTSET alone, and the third indicates their ability to survive both MTSET and osmotic downshock. All V23 data, indicated by a *, is from uninduced cultures due to low viability when induced. Boldface indicates the condition in which the largest and statistically significant decreases in viability are observed. Differences between Osmotic Shock and MTSET are statistically significant ($P < 0.05$ as determined by Student's t test) for Groups I, II, III_a and IV. Differences between MTSET and MTSET + Osmotic Shock are statistically significant for Groups I, III_a III_b, IV, and G30C. Differences between Osmotic Shock and MTSET + Osmotic Shock are statistically significant for Groups II, III_a III_b, IV, and L36C.

Figure 2.1 Viability of Cysteine Mutants Challenged by Osmotic Downshock in the Presence of MTSET

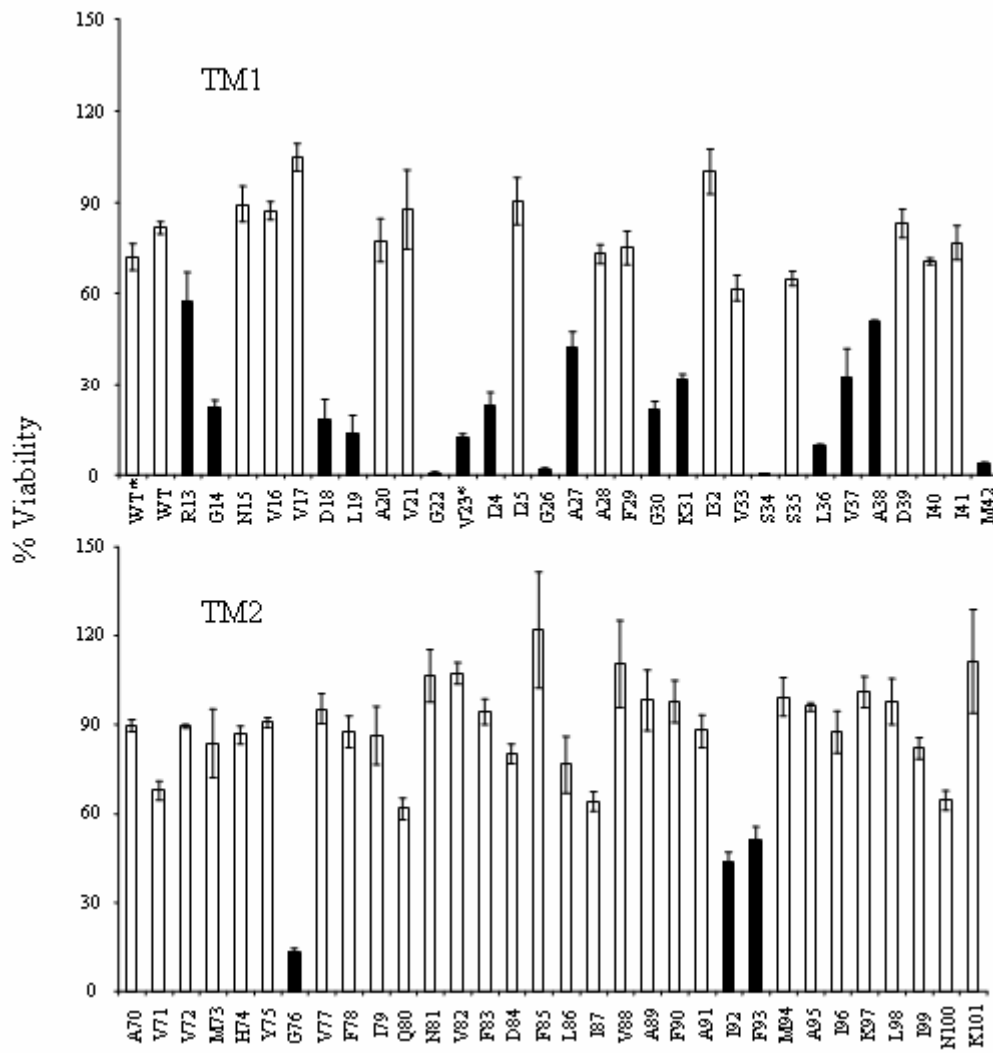


Figure 2.1 Cysteine mutants within the first (Upper, TM1) and the second (Lower, TM2) transmembrane domains were tested. Stars indicate channels that were tested at uninduced levels, WT and V23. Mutants showing <60% viability (filled bars) were targeted for further study. All experiments were performed in duplicate with three to eight independent experiments; SEM for each is shown.

Figure 2.2 Relative position of reactive TM1 residues

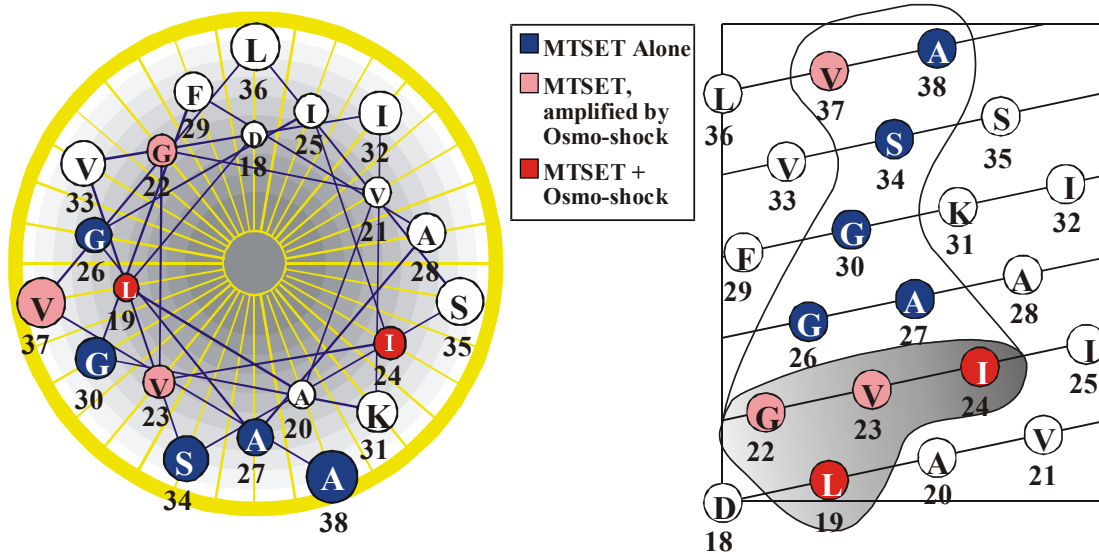


Figure 2.2 An idealized helical wheel (Left) and helical net (Right) are shown. Residues have been colored according to the condition under which decreased viability was seen. Blue indicates that the residues respond to MTSET alone; pink indicates that the residues respond to MTSET alone but show an increased response on osmotic downshock; red indicates that the residues require both MTSET and osmotic downshock to show decreased viability. On the right is the helical net representation of TM1. Enclosed residues react with MTSET; those within the shaded region are residues in the gate that show increased accessibility to MTSET when the channel is gated by osmotic downshock.

Figure 2.3 The Location of Reactive Residues Within Current Models for the Closed MscL Channel

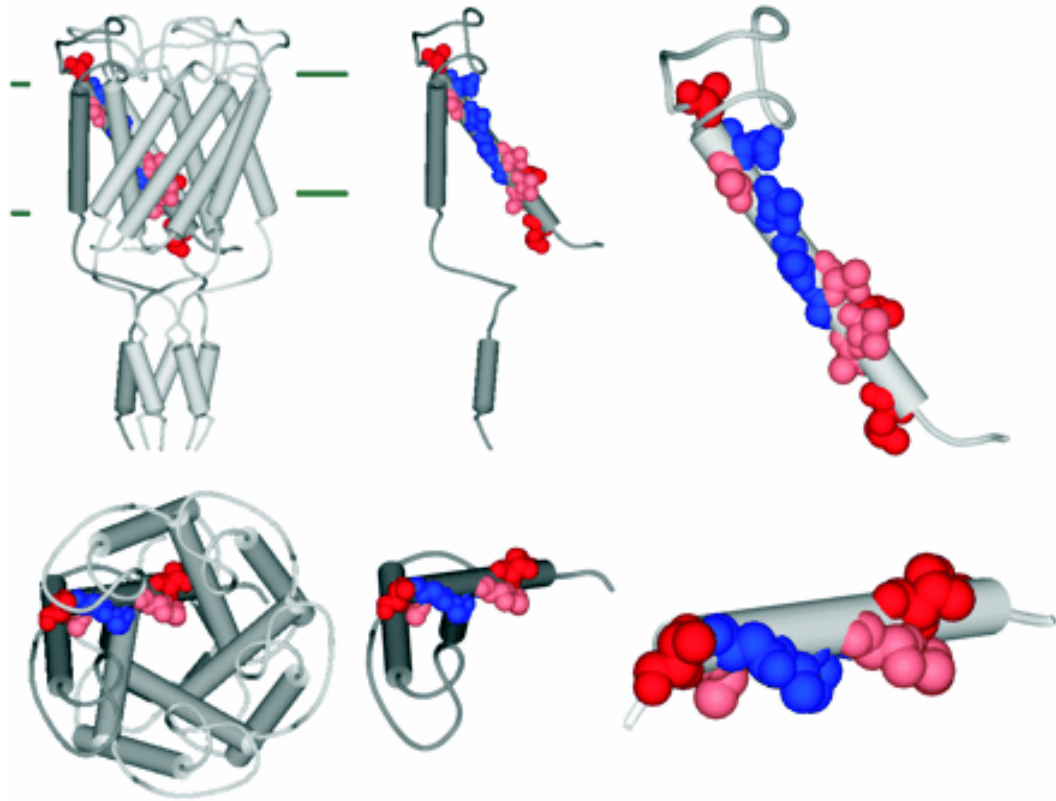


Figure 2.3 The structure of the closed or nearly closed *M. tuberculosis* MscL channel derived from x-ray crystallography is shown. Pictured are profiles of the complex (Left) viewed from the side (Top) and periplasm (Bottom), single subunits (Middle), and a close-up of the TM1 domain (Right). The approximate boundary of the membrane is indicated with green horizontal lines. Residues in TM1 that react with MTSET are shown in CPK format colored according to the condition in which a decreased viability was seen. Blue indicates that the residues respond to MTSET alone; pink indicates that the residues respond to MTSET alone but show an increased response on osmotic downshock; red indicates that residues require both MTSET and osmotic downshock to show decreased viability. Note that in the model the blue-labeled residues are not totally facing the lumen; a slight counterclockwise rotation of TM1 would be required.

Chapter 3 : Mechanosensitive channel gating transitions resolved by functional changes upon pore modification

Introduction

The ability to sense and respond to mechanical stimuli is important for essentially all forms of life. It is not surprising then, that channels responding to mechanical force have now been found in a large number of organisms from archaea to vertebrates (Kloda and Martinac 2001; Sukharev and Corey 2004). Some of the best studied are the bacterial mechanosensitive channels (Sukharev, Blount et al. 1994), which gate in response to tension in the lipid membrane (Moe and Blount 2005). There are three bacterial channel genes that have been identified to encode mechanosensitive activity, the mechanosensitive channel of large conductance (MscL), small conductance (MscS), and K⁺ regulated (MscK; (Sukharev, Blount et al. 1994; Levina, Totemeyer et al. 1999; Li, Moe et al. 2002). MscL was the first to be isolated and is to date perhaps the best studied of all mechanosensitive channels.

Early work showed that the open pore of the MscL channel is on the order of 30Å (Cruickshank, Minchin et al. 1997). Ions, small molecules, and even some

proteins can be released through the pore with little selectivity except by size. In a bacterial cell, the channel discharges small molecules in order to release internal pressure and protect the cell from lysis due to hypoosmotic shock (often called osmotic downshock; (Levina, Totemeyer et al. 1999). Two transmembrane domains were postulated (Sukharev, Blount et al. 1994), and random mutagenesis found that mutations affecting channel gating tended to cluster on one face of the predicted alpha helical first transmembrane domain (TM1; Ou, Blount et al. 1998). When a single residue in TM1, G22, was substituted with 19 other amino acids, it was found that mutations to more hydrophilic or charged residues were found to often cause bacteria to have a severely slow- or no-growth phenotype often times accompanied by a decrease in viability, presumably from the channel gating inappropriately and discharging the proton motive force and cell turgor. (Yoshimura, Batiza et al. 1999). These studies indicated that not only was TM1 vitally important in the kinetics of the channel, but that simply adding a charge or increasing the hydrophilicity of a single residue could drastically affect channel gating and even compromise viability of the cell producing it.

A major advance in understanding came when the *M. tuberculosis* MscL was crystallized to 3.5Å resolution (Chang, Spencer et al. 1998). The crystal structure shows a homopentameric channel with two alpha helical transmembrane domains. TM1 lines the pore while TM2 surrounds the outside of the channel.

There is a 4Å opening in the center of the structure that is insignificant compared to the predicted open pore of 30Å. Therefore, it was postulated that the structure was fully or mostly closed. The crystal structure gave a framework for many of the previous findings derived from both *in vivo* and *in vitro* studies of the *E. coli* MscL. Specific attention was focused on understanding what the open-channel structure might look like and how the channel transitions to obtain an open pore. Two main theories were put forth by Sukharev and Guy (Sukharev, Durell et al. 2001) and by Perozo and Martinac (Perozo, Kloda et al. 2001; Perozo, Cortes et al. 2002). The former model was the first to suggest tilting of the helices as the channel opened, thus matching the thinning lipid bilayer stretched by tension (Sukharev, Durell et al. 2001). The proposed tilting of the helices allowed TM1 alone to form the aqueous pore of the channel, and thus correlated well with the random mutagenesis study demonstrating a clustering of substitutions that effect severe phenotypes in TM1. The model also utilized crosslinking, disulfide-trapping experiments, and computer modeling to predict the open and transitional states of the channel (Sukharev, Betanzos et al. 2001). Subsequently, Perozo and Martinac presented a model based on electron paramagnetic resonance (EPR) studies (Perozo, Kloda et al. 2001). These data were consistent with the tilting of the transmembrane domains and the pore lined by only the first transmembrane domains. However, the residues calculated to line the pore were entirely different. This latter model predicted that TM1 rotated in a relatively drastic clockwise

manner during gating, while the former model indicated a counter-clockwise rotation, thus leading to an almost 180° discrepancy in the orientation of the predicted pore-lining residues.

To determine the residues exposed in the closed and opening states, we utilized the substituted cysteine accessibility method (SCAM; Akabas and Karlin 1999) that we adapted and modified to be a more rapid *in vivo* assay (Bartlett, Levin et al. 2004). This method relied on a previously generated cysteine library (Levin and Blount 2004) and the observation, discussed above, that adding a charge to a single residue within or near the pore, by using the positively-charged sulfhydryl reagent MTSET, can change the gating properties of a channel and, in many instances, severely decrease viability of cells that produce it. The cysteine mutants that demonstrated an MTSET-dependent decreased-viability phenotype fell into three different groups: those that strictly require *in vivo* channel gating, effected by an osmotic downshock, in order to see the phenotype; those that show some MTSET-dependent decrease in viability without an osmotic downshock but require it in order to see the maximal phenotype; and those that do not require any downshock in order to see the MTSET-dependent phenotype. The latter residues were interpreted to compose a periplasmic vestibule while the two former were predicted to be fully or partially buried within the complex and exposed only upon channel gating. This *in vivo* SCAM study gave support for a clockwise

rotation predicted in the model derived from the EPR studies, and defined a number of residues that appear to constitute the pore of the open *E. coli* MscL channel. However, the precise manner in which the channel activity was modified by the MTSET reagent was not determined, and thus any changes in the transition from closed to open states not determined. In this study, the data presented confirm many of our previous predictions as well as give new insight into the structural transitions that occur upon gating.

Results

Utilizing Structural Models and Results from the *in vivo* SCAM to Functionally Subdivide the Pore Domain

The *in vivo* SCAM (Bartlett, Levin et al. 2004) identified regions of the protein likely to be within the closed and opening pore and suggested a classification of the residues identified into three groups: those showing a phenotype in the presence of MTSET alone; those responding slightly to MTSET alone but showing maximum interaction with gating; and those strictly requiring gating in order to interact with MTSET. As seen in **Figure 3.1**, this classification, combined with what is known of the structure of this region, further suggested a functional distinction. The residues that effect a phenotypic change when exposed to MTSET alone (such as G26, G30, and S34) appear to form a vestibule in the

closed structure. The residues that are predicted to be buried and exposed only upon gating (L19, G22, V23, I24, and A27) are lower or more cytoplasmic in the structure. Since MTSET only reacts with cysteines exposed to the aqueous environment, these buried residues would surround the opening or fully open aqueous pore. Residues examined in this study that are predicted to be in the vestibule and those buried and exposed only upon gating are shown in **Figure 3.1** in blue and green, respectively.

Modification of Residues Within the Predicted Periplasmic Vestibule Can Effect Dramatic Changes in Open Dwell Times: G26 AND G30

In the *in vivo* SCAM, cells producing MscL G26C and G30C mutant proteins lost viability when exposed to MTSET, even if the channel was not stimulated to gate by osmotic downshock (**Figure 3.1**; Bartlett, Levin et al. 2004), suggesting that these residues are accessible to compounds in the periplasmic space even without channel gating. Out of the four residues that express this phenotype and are predicted to be within this periplasmic vestibule, G26C and G30C were chosen for study due to their proximity to the proposed constriction site of the closed channel. Because we utilize an inside-out excised patch configuration from native bacterial membranes, we employed a pipette back-fill approach to expose the periplasmic side of the channel to MTSET (Blount,

Sukharev et al. 1996). Briefly, only the tip of the pipette is filled with the patch solution while the rest of the electrode is backfilled with the same solution containing MTSET. Therefore, the patch can be obtained and the ‘untreated’ channel behavior observed before MTSET diffuses into the tip of the pipette and potentially reacts with the channel. The time course for this diffusion is typically about 5-10 minutes. To expose the cytoplasmic side of the patch to MTSET, a concentrated solution of MTSET is simply added to the bath solution. Using these methods, the availability of a residue to the periplasmic (pipette) and cytoplasmic (bath) side of the channel can be tested.

When MTSET was added exclusively to the periplasmic side of the G26C and G30C mutated MscLs, spontaneous openings were observed. In both instances, this gating was seen in a time-dependent manner, as expected from the back-fill procedure described above, and totally independent of any added membrane tension or other mechanical stimulation (**Figure 3.2, Figure 3.3 bottom, and Table 3.1**). For the G26C mutated channel, not only was spontaneous activity observed, but the open dwell time dramatically increased. The first channel opened sporadically, residing in multiple sub-states (**Figure 3.2A**). With time, it “locked” into an open substate approximately 4/5ths the fully open state (**Figure 3.2B and 3.2C**). Each subsequent channel did the same. In these experiments, the patch often exceeds the limit of the recording equipment

after multiple openings. In contrast to G26C, the open dwell time for the G30C mutated channel dramatically decreased when exposed to MTSET on the periplasmic side, and full openings were rarely achieved (**Figure 3.3 bottom**). Hence, while both residues, G26 and G30, appear to be exposed in the aqueous vestibule of the closed channel, reactivity of the cysteine substitutions at these positions have dramatically different effects on channel gating.

G26C and G30C are not, however, accessible to the cytoplasmic side of the channel. As anticipated, when MTSET was added to the bath, the G26C MscL showed no spontaneous openings over the course of several minutes. However, immediately upon gating, the channel showed a gating pattern in which it appears to obtain a 'locked open' state, similar to that observed in **Figure 3.2**. When MTSET is added to the bath of the G30C MscL, no change in the channel kinetics or pressure sensitivity was observed, even after multiple openings (**Figure 3.3 middle**). These data indicate that while neither residue is available to the cytoplasm while the channel is closed, only G26C is accessible to the aqueous pore subsequent to gating; hence, G26C is exquisitely sensitive to modification by MTSET.

**Modification of Residues Within the Predicted ‘Buried’ Region of the Pore
Can Demonstrate Activity-Dependent Changes in Threshold Sensitivity:
V23C and I24C**

The *in vivo* SCAM identified a number of residues postulated to be partially or fully buried within the channel. Of the five residues near the constriction point, V23 and I24 were examined here to further define this area of the channel. Cells producing the V23C MscL mutation in the *in vivo* SCAM showed large differences in viability when treated with MTSET and gated by osmotic downshock (Bartlett, Levin et al. 2004). However, a slight phenotype was also observed in response to MTSET alone, suggesting that there is some reactivity of the reagent with the closed, unstimulated channel. Here, we found that when MTSET was applied to the periplasmic side of a V23C mutated channel, spontaneous sub-state openings were observed after stimulation (**Figure 3.4 bottom**). Surprisingly, however, no activity was observed in the absence of stimulation, even after patches treated on the periplasmic side with MTSET were held for up to 20 minutes.

In contrast to V23, I24C absolutely required osmotic downshock in order for a phenotype to be observed (Bartlett, Levin et al. 2004). Here, we find the threshold pressure to be significantly decreased upon the first opening of the

channel; the pressure required to gate MscL compared to MscS decreased from 1.73 ± 0.06 to 1.23 ± 0.04 (**Figure 3.5 top and bottom and Table 3.1**).

Neither V23C nor I24C appear to react with MTSET applied to the cytoplasmic side. Even when these channels were gated with MTSET present in the bath, neither kinetics nor threshold pressures changed (**Figure 3.5 middle** and data not shown). These data are consistent with the hypothesis that V23C and I24C are buried and are only available from the periplasmic side when the channel is gated.

Discussion

Previous studies screening randomly mutated libraries of MscL have demonstrated that mutations in and around the pore of the channel can lead to severely compromised growth and viability of cells expressing the mutated protein (Ou, Blount et al. 1998; Maurer and Dougherty 2001). In one study, electrophysiological characterization of the mutants demonstrated a correlation between the severity of the slow- or no-growth phenotype, a leftward-shift of the activation curve (the mutant channels were more sensitive to stimulus) and a decrease in the open dwell time of the channel (Ou, Blount et al. 1998). In a subsequent study, a single residue, G22, was substituted with the 19 other amino

acids; this study demonstrated that the more hydrophilic the substitution in this region, the more severe the *in vivo* and channel phenotypes observed (Yoshimura, Batiza et al. 1999). The leftward shift of the sensitivity curve, coupled with the severely shortened open dwell times suggested that hydrophilic substitution allowed the channel to transition between a closed and open conformation more easily, which in turn led to a channel that opened at lower tensions and spent less time in the fully open conformation. At a more mechanistic level, these findings led to the proposal that at some point in the opening of the channel this residue must pass through or reside in a hydrophilic micro-environment; the residue is thus likely to be in a more hydrophobic environment in the closed position. Changing the hydrophilicity of a residue can also be accomplished post-translationally by mutating a residue to a cysteine and then allowing it to react with a charged MTS reagent, such as MTSET. Indeed, using this approach, consistent results for the previous G22 study, discussed above, have been obtained (Yoshimura, Batiza et al. 2001). Other studies have also utilized the positively charged MTSET to identify residues within the proposed pore domain that are exposed either in the closed (presumably in a periplasmic vestibule) or opening states within a cellular context; this approach has been coined the *in vivo* SCAM (Yoshimura, Batiza et al. 2001; Batiza, Kuo et al. 2002; Chapter 2). Here we have examined a number of mutated channels modified by this technique using electrophysiological approaches that allow us to measure the kinetics and

sensitivity of the channel. Our data support many aspects of previous models of the transition states and structure of the open channel, but they also give a new higher resolution of the pore domain and its transition from the closed to open state.

Adding the charged sulfhydryl reagent MTSET at positions G30, V23 and I24 led to channel activities that not only gated at lower stimulus but also demonstrated drastically decreased open dwell times. Previously, the same modifications of two additional pore mutations, L19 and G22, yielded similar results (Yoshimura, Batiza et al. 2001; Batiza, Kuo et al. 2002). These findings may reflect a combination of two effects. First, the placement of a charge in these positions drastically changes the hydrophilicity of the region; the change seen in activity could be because the residues normally encounter an aqueous environment during gating, and an increase in hydrophilicity enhances the probability of this transition. Second, if more than one of the subunits within the pentameric complex are modified, one would expect electrostatic repulsion due to the proximity of these residues within the lumen of the channel. In either event, these changes could lead to either the destabilization of the closed and open states and/or stabilization of the transition states of the channel, and thus a channel with short open dwell times.

The requirements for MTSET accessibility to specific residues give clues to the microenvironment of the residue in different states of the channel. For residues L19C and G22C in the closed conformation either *in vivo* (Bartlett, Levin et al. 2004) or patch clamp (Yoshimura, Batiza et al. 2001; Batiza, Kuo et al. 2002), strong influences are observed subsequent to channel gating; the results strongly suggest these residues are buried in the closed state and exposed only upon channel gating (Yoshimura, Batiza et al. 1999; Batiza, Kuo et al. 2002). In support of the data obtained from the *in vivo* SCAM study, we find that G30 and G26 do not require any gating to observe dramatic changes in channel activity when treated with MTSET. In contrast, maximal effects of MTSET treatment were observed for V23 and I24 only subsequent to osmotic downshock. Interestingly, in patch clamp, channel gating was an absolute requirement for changing the channel activity of V23C, whereas the *in vivo* experiments suggested some accessibility independent of stimulation by hypo-osmotic treatment (Bartlett, Levin et al. 2004). A likely explanation is that the *E. coli* cytoplasmic membrane has enough tension to gate V23C *in vivo*. Consistent with this interpretation, production of MscL V23C in a cell leads to a slowed-growth phenotype (Levin and Blount 2004), presumably due to promiscuous gating even in the absence of osmotic downshock. As previously noted (Chapter 2), the exposure of I24 to the lumen of the pore would require a clockwise rotation of TM1 during the gating process. Again, consistent with the *in vivo* SCAM, we

found that MTSET treatment in the presence of gating led to a channel that gated at a lower threshold. However, given the predicted ‘buried’ nature of this residue, it is puzzling that this change in sensitivity is observed with the first opening. A clue for the resolution of this apparent paradox is obtained from another study demonstrating that the exposure of the I24 residue to the pore may occur prior to ion permeation. Briefly, the previous study demonstrated that an I24H mutant apparently bound to heavy metals including Ni^{++} and Zn^{++} , which lead to a ‘locking’ into the closed state of the channel. This would occur if the putative clockwise rotation of the TM1 domain occurred prior to ion permeation. Our data would be consistent with this interpretation; although channel activity is not observed in patch while the tension is sub-threshold; one or more of the TM1s may be rotating as a precursor for gating, thereby exposing I24 to a position of accessibility. Together the data strongly suggest that TM1 makes a clockwise rotation to expose I24 during the normal gating process prior to ion permeation, and that the amount of tension in the *in vivo* cytoplasmic membrane is sub-threshold for this motion, yet greater than the threshold for gating of the V23C mutated channel.

G26C demonstrated the most unique properties for both its accessibility to, and kinetic changes upon, modification with MTSET. This residue was first proposed to be the possible constriction point of the *E. coli* MscL channel when it

was shown that G26C tends to form disulfide bridges and is difficult to see in patch clamp without DTT, indicating that the residues are close to each other in the closed conformation (Levin and Blount 2004). A metal binding study also provided evidence that G26 residues are positioned in such a manner that they, not V23, should be the constriction point (Iscla, Levin et al. 2004). Consistent with this hypothesis is the observation in this study that G26C, when modified by MTSET, resides largely in an open state. As seen in **Figure 3.2**, this channel phenotype is not immediately observed, but instead the channels first show ‘flickery’ spontaneous activity, then acquire a ‘locked’ open state. These data suggest that the binding of more than one MTSET per pentameric complex is required for the open-state channel phenotype. If these residues are truly of closest proximity, then electrostatic interactions may be keeping the channel open. The fully open conductance, however, is not easily obtained, instead, the channel appears stabilized in a 4/5ths sub-conducting state. This reflects an inability of achieving the final open state, perhaps because a full rotation of the TM1 domain normally buries G26, and this structure cannot be easily achieved because of steric or energetic constraints due to the charge now associated with the residue. Finally, G26C was the only residue in this study that showed accessibility, upon gating, to the cytoplasmic side of the channel. Although L19C (Batiza, Kuo et al. 2002) and G22C (Yoshimura, Batiza et al. 2001) have previously also been shown to be accessible from the cytoplasmic side upon gating, G26C remains the most

periplasmic residue that, upon gating, is available to the cytoplasmic application of an MTS reagent. Together, these data argue for a very unique role and positioning of the G26 residue in the closed, open and transition states of the channel.

Figure 3.1 Schematic Depictions of the *E. coli* MscL Emphasizing the Pore Domain and Specific Residues that were Targeted for Substitutions

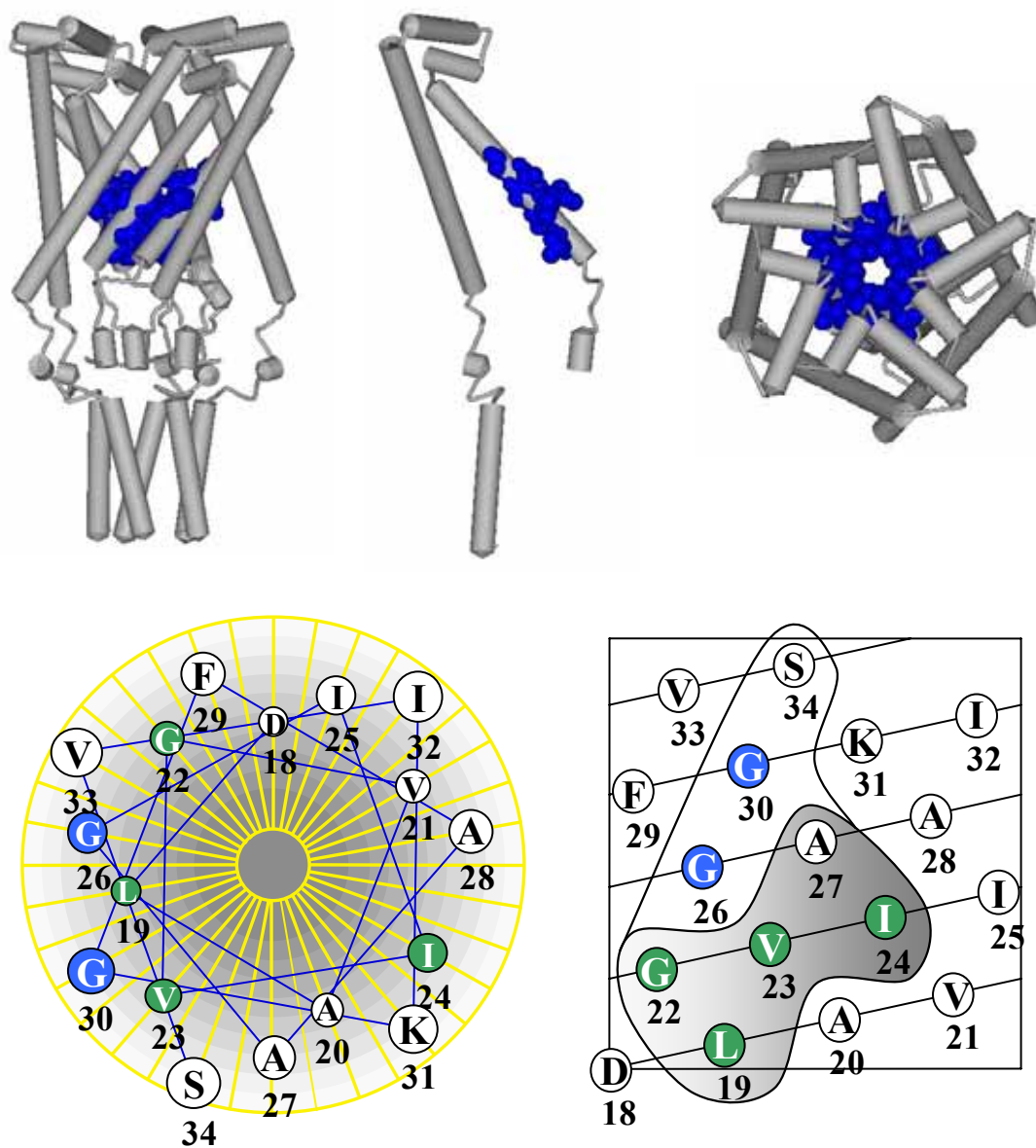


Figure 3.1 The upper panel shows a model for the closed MscL structure (Sukharev, Durell et al. 2001) based upon the crystal structure (Chang, Spencer et al. 1998). The residues investigated by this study are highlighted in blue and shown in a cpk format. A side view (left), a single subunit of the pentameric complex (center) and top view are shown. The bottom panel presents an idealized helical wheel (left) and net (right) of the *E. coli* MscL first transmembrane domain. The residues encircled in the helical net were identified in the *in vivo* SCAM assay (Bartlett, Levin et al. 2004) as described in text. The residues within the shaded region were accessible to MTSET only upon channel gating by osmotic downshock. The residues that are further investigated by patch clamp in this study are colored dependent on whether the MTSET was accessible without (blue) or with (green) channel gating.

Table 3.1 Channel Activity in the Presence and Absence of MTSET

Residue	No Treatment	MTSET in the pipette (Periplasmic side)	MTSET in the bath (Cytoplasmic side)
G30C	1.62 ± 0.07	Spontaneous Activity Independent	1.65 ± 0.09
G26C	ND	Spontaneous Activity Independent	Spontaneous Activity Dependent
I24C	1.73 ± 0.06	1.23 ± 0.04 Activity Independent*	1.75 ± 0.07
V23C	0.90 ± 0.17	Spontaneous Activity Dependent	0.72 ± 0.07
G22C†	1.9 ± 0.9	Spontaneous Activity Dependent	Spontaneous Activity Dependent
L19C‡	0.78 ± 0.27	Spontaneous Activity Dependent	Spontaneous Activity Dependent

Shown is the threshold \pm SEM. The threshold is presented as the ratio of the pressure required to open MscL over the pressure required to open MscS in the same patch as previously described (Blount et.al., 1996). $N \geq 3$. “Spontaneous” indicates conditions where activity is observed independent of a pressure stimulus, and changes in channel activity due to MTSET treatments are noted to be dependent or independent on channel gating. ND – Not Determined.

*The change in threshold was seen with the first opening of the channel.

†Data from (Yoshimura et.al, 2001).

‡Data from (Batiza et. al., 2002).

Figure 3.2 G26C Locks in an Open Channel Conformation When Modified by MTSET Placed on the Periplasmic Side

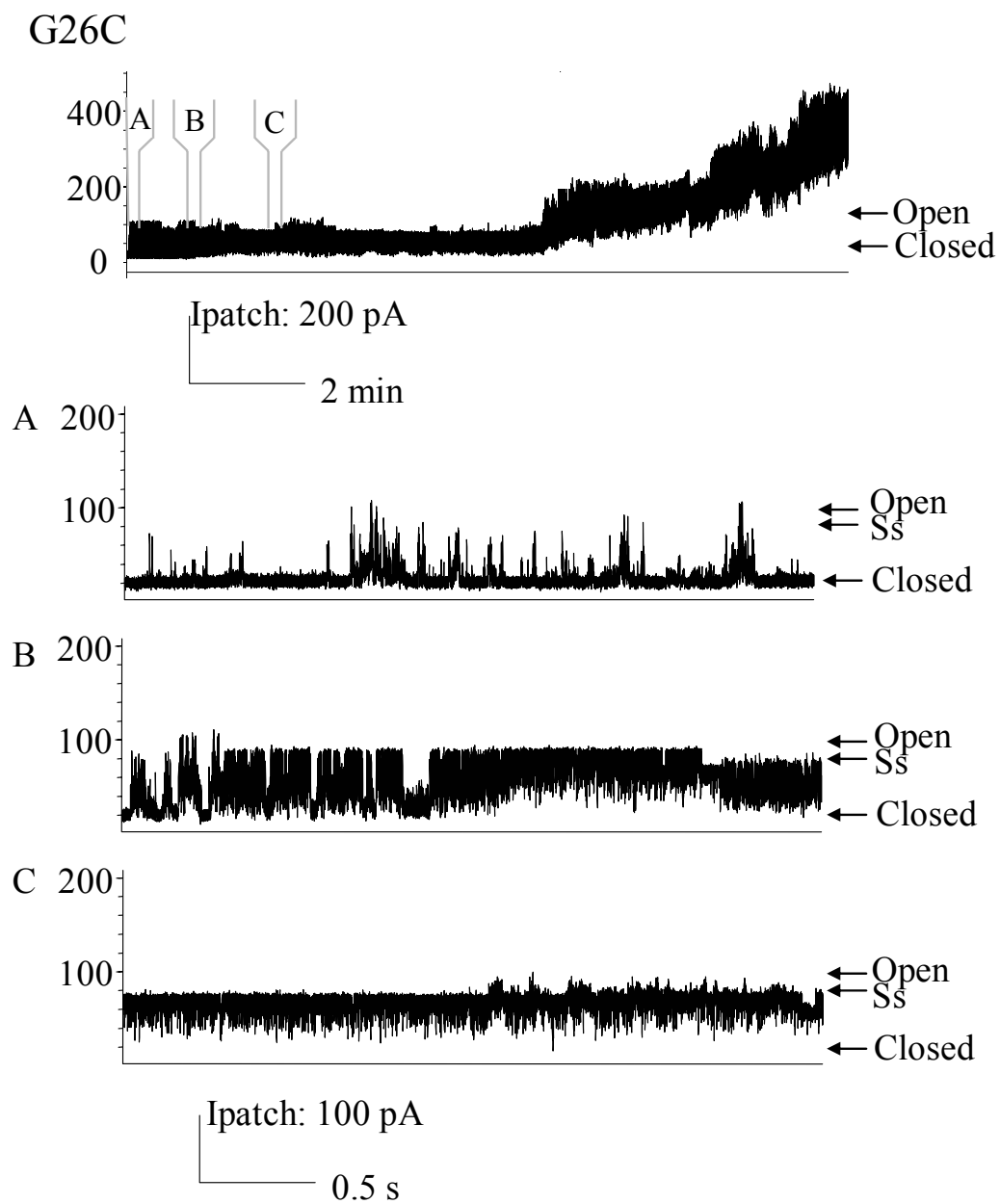


Figure 3.2 The uppermost trace shows G26C activity with MTSET added by backfilling the pipette as described in Materials and Methods, note that no pressure was applied before or during this trace. At the time points indicated by A, B, and C, the trace has been expanded. Section A shows the first channel starting to open and the preference for substates and short open dwell times. Section B shows the first channel being locked into an open state. Section C shows the final preference of the channel for a common 4/5th open substate.

Figure 3.3 G30C Shows Gating-Independent Spontaneous Activity When Modified by MTSET Placed on the Periplasmic, but Not Cytoplasmic Side

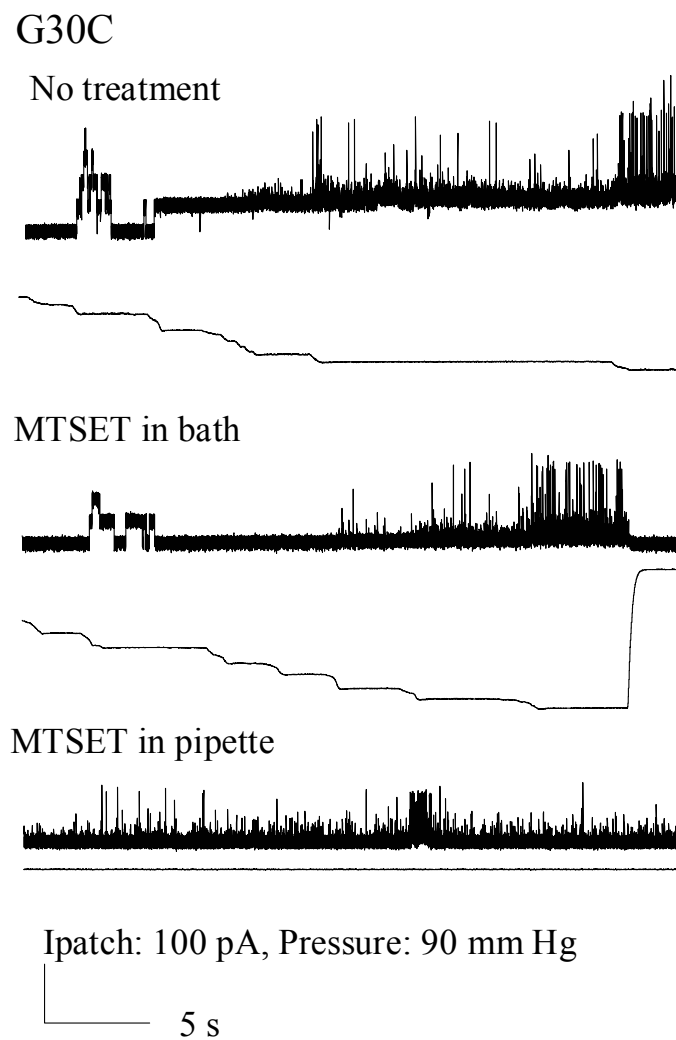
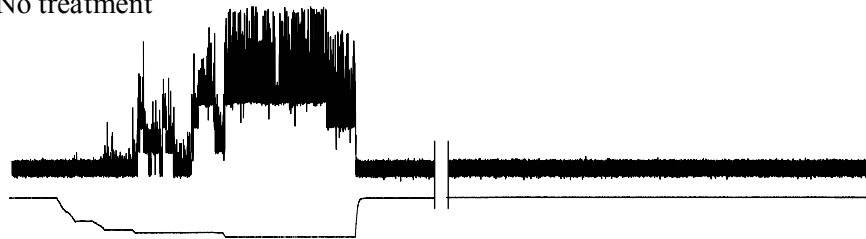


Figure 3.3 Single channel recordings of G30C are shown from top to bottom without treatment, with MTSET added to the bath, and with MTSET added to the periplasmic side of the patch by backfill, as described in text. In the final trace, G30C shows spontaneous gating, only rarely obtaining a fully open state.

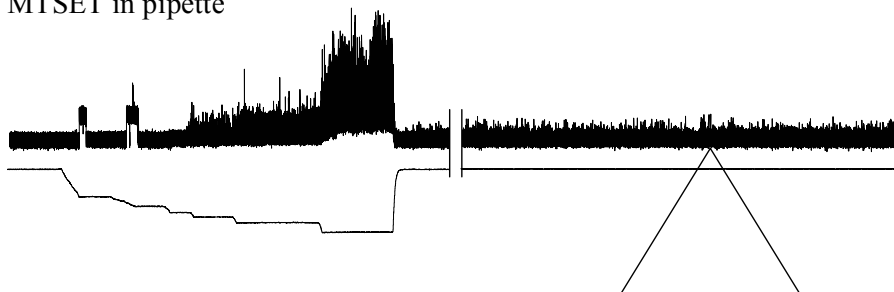
Figure 3.4 V23C Shows Gating-Dependent Spontaneous Activity When Modified by MTSET Placed on the Periplasmic, but Not Cytoplasmic Side

V23C

No treatment



MTSET in pipette



Ipatch: 50 pA, Pressure: 120 mm Hg

5 s



Ipatch: 50 pA

0.5 s

Figure 3.4 Single channel traces of V23C show spontaneous openings upon the combination of gating and addition of MTSET to the periplasmic side. A trace is shown before interaction with MTSET (top) and after MTSET has diffused into the pipette solution using the backfill method (bottom). Hash marks represent ~3-5 min removed to show durability of response. Note the rapid and incomplete openings in the expanded trace, right hand side on the bottom.

Figure 3.5 I24C Shows Gating-Independent Increased Sensitivity When Modified by MTSET on the Periplasmic, but Not Cytoplasmic Side

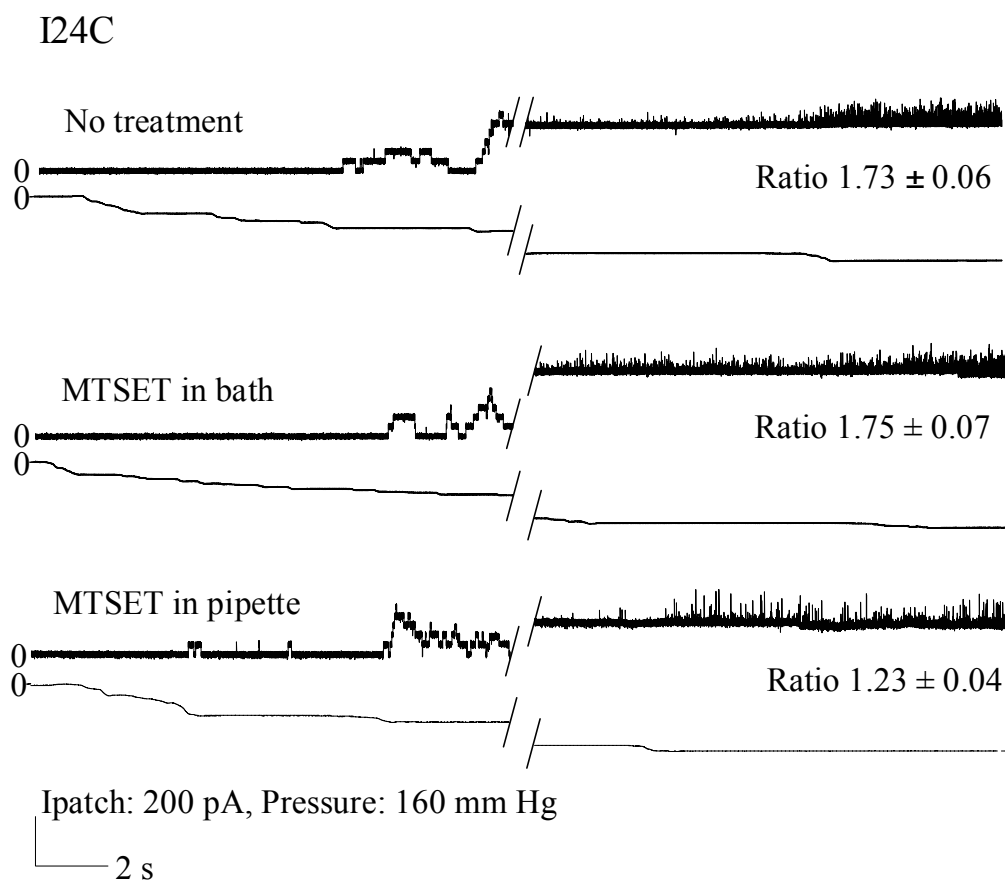


Figure 3.5 Single channel recordings of I24C illustrate the change in pressure sensitivity upon addition of MTSET on the periplasmic side. The 'ratio' is the ratio of the relative pressures for opening MscL/MscS, as described in Materials and Methods; a larger ratio indicates a channel that requires more tension to open. The first or topmost trace is I24C with no treatment. The second trace is the same patch with MTSET added to the cytoplasm and it has been exercised multiple times. The third trace is obtained where the pipette was backfilled with MTSET as described in Materials and Methods. Hatch marks indicate 20-30 seconds removal of MscS activity.

Chapter 4 : Understanding the structural differences between MscL orthologues and how these differences lead to functional variations

Introduction

Mechanosensitive channels are a uniquely adapted type of channel, conveying mechanical stimuli into a cellular signal or response. Their function is considered to be vitally important since most organisms, including microbes, contain at least one type of channel that responds to mechanical stimulation. One of the best studied is the bacterial mechanosensitive channel of large conductance (MscL). In *E. coli*, the channel senses tension within the membrane and functions as an emergency release valve to protect the cell from lysis due to hypoosmotic shock (Levina, Totemeyer et al. 1999). While there is some redundancy with other mechanosensitive (MS) channels performing the same function, production of the *E. coli* (Eco) MscL channel is sufficient to rescue an *E. coli* cell devoid of the other major MS channels from lysis due to such an osmotic downshock (Levina, Totemeyer et al. 1999). Since the isolation and characterization of Eco MscL (Sukharev, Blount et al. 1994), many homologues have been found. To date, over ten homologues have been shown to be functional, encoding MS channel activities (Jones, Naik et al. 2000; Kloda and Martinac 2001; Nazarenko,

Andreev et al. 2003; Folgering, Moe et al. 2005). Studies have also shown that production of these MscL orthologues from other bacterial species often protects an osmotically fragile *E. coli* strain (Moe, Levin et al. 2000), null for MscL and lacking another MS channel named MscS (Levina, Totemeyer et al. 1999; Moe, Blount et al. 1998; Folgering, Moe et al. 2005). Hence, many of these proteins appear to be fully functional orthologues with indistinguishable cellular function.

There are four parameters normally measured when characterizing a bacterial MS channel: its ability to function properly in a cell (growth and protection from lysis), the threshold tension (how much tension is required to open the channel), the channel kinetics (how quickly the channel can transition between an open and closed state), and the conductance (the size or shape of the open pore). The first cellular phenotype associated with the channel was identified when point mutations were discovered that lead to a slowed- or no-growth phenotype (Ou, Blount et al. 1998). This gain-of-function (GOF) phenotype was proposed to be due to the channel gating inappropriately *in vivo*. The *in vivo* loss-of-function (LOF) of the channel, mentioned above, leads to cell lysis upon osmotic downshock. These two phenotypic assays (decreased growth rate when a mutant or orthologue is expressed, which we will refer to as a GOF assay, and survival upon osmotic downshock, referred here as the osmotic lysis assay) form

the gold standard by which MscL channel function is measured within a cell. Patch clamp, on the other hand, gives the intimate details, such as the kinetics and conductance of a single channel activity *in vitro*. Together, these methods provide a clear image how a channel functions or misfunctions. Even with these powerful approaches, questions of how the channel transitions from a closed conformation into the very large open pore still abound. Specifically, it remains unclear what the contribution of each domain is towards controlling the pore shape and size, channel kinetics, and sensitivity.

A leap forward in understanding channel structure came when *M. tuberculosis* (Tb) MscL was crystallized to 3.5Å (Chang, Spencer et al. 1998). The channel is made up of two alpha helical transmembrane domains with the first transmembrane domain forming the pore and the second transmembrane domain forming the outer portion which interacts with the lipids. While *E. coli* and *M. tuberculosis* are from very different bacterial families, they contain MscL sequences 29% identical and are thought to be very similar in structure. A model for the *E. coli* MscL has been derived from the Tb crystal structure (Sukharev, Durell et al. 2001) which places the N and C termini within the cytoplasm with a periplasmic loop connecting the two transmembrane domains. The N-terminus (S1), which was not resolved in the crystal structure, was modeled as a helical

bundle. Similarly, the first transmembrane domain (TM1), periplasmic loop, second transmembrane domain (TM2), and cytoplasmic C-terminus also appear to be helices. Sukharev et. al. also modeled the TM1 to form the pore of the channel in several stages of gating. This model has provided a simple delineation between domains of the channel.

Surprisingly, expression of the Tb MscL homologue fails to save an osmotically fragile *E. coli* cell line (Moe, Levin et al. 2000). When examined in patch clamp, Tb MscL also has a change in the threshold tension, but maintains similar kinetics and conductance to Eco MscL (Moe, Levin et al. 2000). Due to the plethora of data accumulated for both Eco and Tb MscL channels, as well as the easily tested functional difference within cells, these two channels seemed ideally suited for chimeric analysis to determine the structural properties leading to these functional differences. Similarly, functional differences in channel kinetics and conductance are observed between Eco MscL and *S. aureus* MscL (Sau), which are 45% identical (Moe, Blount et al. 1998). Hence, an understanding of structural influences over these channel properties can be obtained by generating chimeras between these orthologues. The chimeras constructed between Eco and Tb and Eco and Sau MscLs have given insight into

structural domains that can alter channel threshold tension, kinetics and conductance.

Results

The S1/TM1 Region of MscL Contributes to Stimulus Sensitivity

To identify structural elements that contribute to the observed differences in channel threshold sensitivity, chimeras were constructed between Eco MscL and Tb MscL. The chimeras were constructed using multi-round PCR reactions (as described in Chapter 5) with the junctions in conserved regions. Briefly, portions of the parental channel DNA were cloned with overlapping sequences consistent with the second portion of the chimera channel. The two DNA portions of the final sequence were then ligated to each other using the overlapping portions, and external primers amplified the complete sequence. Tb MscL was chosen for chimeras with Eco MscL because the crystallization of the channel (Chang, Spencer et al. 1998) gave us a detailed structural framework and because previous experiments showed it has a dramatically decreased sensitivity to stimuli (Moe, Levin et al. 2000). In patch clamp experiments, Tb MscL required greater than two times as much tension in order to stimulate opening as that of Eco MscL, and in an *in vivo* osmotic downshock assay, production of the channel was insufficient to protect the cell from lysis (Moe, Levin et al. 2000). Here, we used

this latter *in vivo* assay to measure the threshold sensitivity of MscL chimeric channels by testing their ability to function in the osmotic lysis assay.

There is a strong correlation between the *in vivo* function of the protein and the S1/TM1 domains of the protein. Data presented in **Figure 4.1** and **Table 4.1** show that of all of the chimeras generated between Eco and Tb MscL, only those containing the S1/TM1 domains from the Eco MscL (ET1, ET2 and ETL) were functional as tested by the osmotic lysis assay. ET2 contains an additional portion, the periplasmic loop of Eco MscL, while ETL lacks the loop and contains the TM2 and C domains. Notice that for ET1 and ET2, the majority of the sequence is derived from Tb MscL, which is non-functional in this assay. The converse chimeras (TE1, TE2 and TEL) also follow the trend of TM1 setting the channel sensitivity to stimuli. Since the S1/TM1 domains changed the functionality of the channel, we tested the possibility that a smaller region of the protein was responsible for the change; hence, ET29 and T29E40 were created. ET29 contains the S1 and first half of the Eco MscL TM1 on a Tb background, while T29E40 contains the second half of Eco MscL TM1. Neither ET29 nor T29E40 were functional as assayed by their ability to suppress the osmotic lysis phenotype. Hence, although the threshold sensitivity of the channel cannot be isolated to a few residues within S1/TM1, it is clear that the S1/TM1 domains

play an important role in transducing the tension stimuli into the opening of the channel.

The *S. aureus* MscL Channel Suppresses the Osmotic Lysis Phenotype

S. aureus mscL has previously been shown to encode a MS channel activity within a bacterial membrane (Moe, Blount et al. 1998). Here we also show that the channel is able to function as an osmotic safety valve for the cell during hypoosmotic stress. In an osmotically fragile *E. coli* cell line, expression of the *S. aureus* MscL (Sau) is sufficient to rescue the lysis phenotype in a manner similar to the *E. coli* MscL (**Table 4.2**).

The S1/TM1 Domains Play a Role Determining the Kinetics of the Channel While the Second Transmembrane Domain Can Influence Conductance

There are significant differences in channel kinetics between *E. coli* MscL and *S. aureus* MscL. This finding has led us to focus on these two channels as interesting foils for each other that could give insight into the overall function of each domain in the channel in forming and maintaining the open structure. Since kinetic differences have previously been observed primarily in TM1 mutations (Ou, Blount et al. 1998), the S1/TM1 and loop domains were swapped as in the Eco-Tb chimeras (see **Figure 4.2**). When the channel sensitivity was examined

using the *in vitro* patch clamp method, an interesting division of the chimeras was observed. The chimera containing the S1/TM1/loop of Eco MscL (ES2) had kinetics indistinguishable from Eco MscL, while the τ_3 of a chimera containing only the S1/TM1 region, ES1, is also significantly longer than that of Sau MscL. Once open, this channel has a tendency to ‘flicker’ into a closing state; hence, without this bursting behavior it is visually comparable to Eco MscL and has therefore been categorized with the longer open dwell time channels. By contrast, the chimera containing the S1/TM1 of Sau MscL (SE1) had kinetics similar to Sau MscL (**Figure 4.2, 4.3, and Table 4.2**). These results show a correlation between the S1/TM1 region and channel open dwell times.

Careful measurements of the Eco and Sau MscL channels also show that these channels have a measurable difference in conductance, which correlates with the size and shape of the pore. Measuring the conductance of the chimeras demonstrates that the TM2/C-term domains play a role in this property (**Figure 4.3, 4.4, and Table 4.2**). The SE2 chimera, which contains the S1/TM1 and loop domains of Sau MscL and the TM2 and cytoplasmic domains of Eco MscL, was also constructed, but because the threshold of gating the channel was very high, useful data could not easily be obtained. This may be due to a loss of stimuli sensitivity; SE2 showed a decreased ability to function within the *in vivo* osmotic

lysis assay and therefore presents a classic loss-of-function phenotype (**Table 4.2**). When the other chimeras were examined, ES1 and SE1 were able to rescue the lysis phenotype (**Table 4.2**). ES2 was not examined within this assay because its expression caused a slow growth phenotype within the cell, which would complicate any results observed (data not shown).

Discussion

Since *E. coli* MscL has been isolated and characterized, a number of functional orthologues, have been identified. However, many of them showed functional differences when produced in *E. coli*. Here the underlying structural basis for the functional differences between orthologues is dissected in order to determine the contribution of each domain toward the overall function of the channel. Areas of high conservation were chosen for junction points in order to minimize misfolding or misassembly. The S1/TM1 domains were shown to contribute to the sensitivity and kinetics of the channel in responding to stimuli both *in vivo* and *in vitro*. Furthermore, the TM2/C-terminal domain appears to play a role in setting the shape or size of the open pore.

Our data further refines the role the N-terminal region of the protein plays in channel gating. TM1 has been shown repeatedly to influence gating properties. Mutagenesis studies mapped severe gating mutants to the proposed helical face of

TM1 (Ou, Blount et al. 1998). These gating mutants, which were primarily substitutions to more hydrophilic residues and often added a charge, changed the threshold for the opening of MscL and the channels often exhibited a shorter open dwell times. Similarly, in studies in which TM1 was altered using a Substituted Cysteine Accessibility Method assay (SCAM – see previous chapters; Batiza, Kuo et al. 2002), a correlation was often noted between increased channel sensitivity and short open dwell times. This allowed a rapid identification of residues that demonstrated a change in channel function simply by the addition of a charge at that position (See Chapter 2). While short open dwell times of mutant MscL channels have often been correlated with an increased sensitivity that frequently leads to a decrease in cell growth upon induction of channel expression, one does not always predict the other. The two orthologues chosen for this study exemplify the disconnection of channel sensitivity and kinetics; Tb shows an altered sensitivity or threshold and Sau altered kinetics without much change in sensitivity. Our data from the Eco and Tb MscL chimeras clearly indicate that N-terminal half of the molecule, including S1 and TM1, plays a significant role in setting the threshold sensitivity: the observation that the function does not correlate easily with sub-domains (see Figure 4.1 bottom two right most panels) indicates that more than one residue or region is involved in the functional differences observed.

The kinetic differences observed between Eco and Sau MscL also mapped to the S1/TM1 domain. By comparing the amino acid sequence of the protein the possible changes that would effect gating are not obvious. Out of the 13 S1/TM1 residues that are different, only three seem to be non-conserved substitutions (G22>A, A38>E, and D39>N). A G22A substitution has been made previously in Eco MscL, and while both G and A are both small residues, that previous study demonstrated that with this minor change the channel had much longer open times, not shorter (Yoshimura, Batiza et al. 1999). While residues A38 and D39 have never been isolated in random or site directed mutagenesis studies, it may be important to note that the former is the gain of a charge while the latter loses one. As discussed above, previous studies have often correlated the gain of a charge with channel misfunction, including shorter open dwell times (Ou, Blount et al. 1998). In addition, A38 was previously mutated to a cysteine and exposed to MTSET in the SCAM assay (Chapter 2). The cysteine mutation had no effect on viability, but the addition of a positive charge at that residue, via the charged sulfhydryl reagent MTSET, significantly decreased the ability of the cells to grow. Since most of the modifications leading to this phenotype are correlated with shorter open dwell times of the channel, it seems possible that this residue plays a role in the effects observed. While it is unlikely that the single A38 residue is solely responsible for the kinetic differences observed between Eco and

Sau MscL, it would be a simple and informative substitution to carry out in the future.

The periplasmic loop domain of MscL, based on our experiments, may play a role in maintaining the closed structure, even though the loop is not necessary for transduction of membrane tension into channel gating. A recent study by Park, *et. al.* indicated that interactions between the transmembrane domains were responsible for the transduction of tension within the channel when they produce the N-terminal and C-terminal regions of MscL as separate proteins (Park, Berrier et al. 2004). However, the channels they reconstituted gated at an increased sensitivity. In a similar manner, when a protease is placed on the periplasmic side of the channel to digest the periplasmic loop, a MscL channel activity that gated more easily in response to membrane tension was observed (Ajouz, Berrier et al. 2000). Our data, showing differences between two Eco-Sau chimeras, ES1 and ES2, are consistent with the idea that the loop region plays a role in the elasticity or as an internal ‘spring’ of the channel. Note that ES1, which contains the loop domain from Sau MscL, has open dwell times between and different from both, the Eco and Sau MscL; however inclusion of the Eco MscL loop in ES2 (**Figure 4.3**), generates a channel with kinetics indistinguishable from the Eco MscL. Hence, it appears that the periplasmic loop domain can play a role

in defining channel open dwell times, presumably because of its 'spring-like' qualities.

A number of MscL homologues have been studied, and using patch clamp it has been demonstrated that they form mechanosensitive channels with a range of conductances, anywhere from 2-4nS (Moe, Blount et al. 1998). While Sau MscL had been patched previously, due to its fast kinetics a unitary conductance had not been calculated. While Sau MscL was initially chosen for this study because of its kinetics, probably the most interesting information to be obtained from these chimeras came from the markedly different conductances. The conductance reported here for Sau MscL could be a slight underestimate due to the extremely short open dwell times, but every effort was taken to choose 'square' channel openings in this determination. The observation that the TM2/cytoplasmic bundle seems to set the pore size was unexpected, but upon examination not unlikely. While we cannot rule out the possibility that the cytoplasmic bundle is responsible for the pore size, much of the cytoplasmic C-terminus has been previously removed and channels were observed with a conductance indistinguishable from Eco MscL (Blount, Sukharev et al. 1996), making it more likely that TM2 alone is responsible for the conductance change. In addition, the length and much of the sequence is conserved between the two

orthologues (Pivetti, Yen et al. 2003). On the other hand, TM2 has been observed in the crystal structure to form the outer portion of the channel which would interact with the lipid environment in the closed conformation (Chang, Spencer et al. 1998) and is modeled to form the outer portion of the channel in the open conformation as well (Sukharev, Durell et al. 2001). As mentioned previously, a study was carried out in which the N- and C- terminal portions of MscL were produced separately and patched looking for activity (Park, Berrier et al. 2004). The results from that study are consistent with TM2 setting the conductance or size of the channel because the N-term expressed alone formed channels with multiple conductances, but the combination of the two transmembrane domains consistently produced a channel with an invariant conductance consistent with the wild type channel. The TM2 may control the size by specific protein-protein interactions with TM1, or it may expand independently of TM1 through interactions between other TM2 helices and interactions with the membrane. While we cannot distinguish between these two possibilities, molecular modeling studies have indicated that there may be a pre-conducting expansion of the channel within the membrane (Sukharev, Betanzos et al. 2001). This expansion has been cited in order to support a model in which the N-terminus S1 forms a secondary gate in the channel. However, functional data seems to support a single gate within the channel (Hamill and Martinac 2001) and based on this data the pre-gating expansion could possibly be due to the movement of TM2 instead of

TM1 as previously proposed. Consistent with this hypothesis, a molecular simulation study by Columbo *et. al.* indicated that TM2 expanded before TM1 during gating in order to create a space for TM1 to occupy (Columbo, Marrink et al. 2003). Regardless of what interactions set pore size, the observation that TM2 may play a role in setting the channel conductance opens up a new line of study that should be investigated.

Figure 4.1 Cell Survival Follows the S1-TM1 Domain

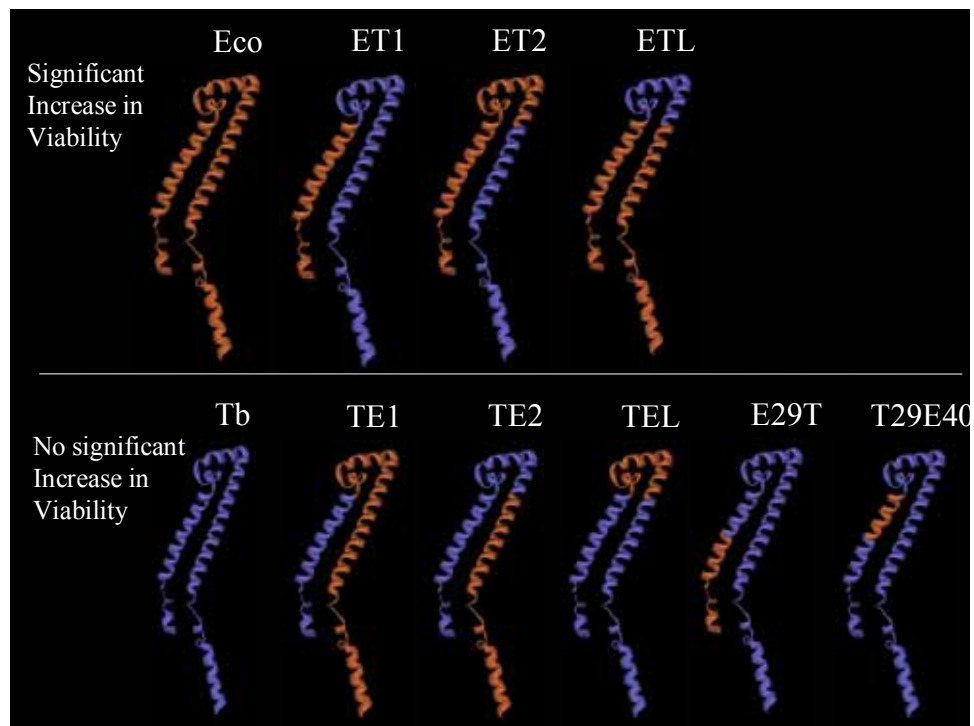


Figure 4.1 The S1/TM1 of MscL contributes to the ability of the channel to save the cell from hypo-osmotic shock. A pictorial representation of a chimera subunit based upon the *E. coli* MscL models is presented. Eco-Tb chimeras are divided into two groups, those that significantly save the cell as compared to empty plasmid and those that do not.

Table 4.1 Quantification of Rescue in *in vivo* osmotic lysis assay

Strain	Normalized % Viability
Plasmid	0.00 ± 0.0
Eco	100.0 ± 0.0**
Tb	-0.28 ± 2.52
ET1	49.19 ± 12.36**
ET2	29.26 ± 11.73**
TE1	-3.71 ± 1.17
TE2	4.56 ± 4.87
E29T	5.18 ± 1.20
T29E40	-2.49 ± 1.65
ETL	6.33 ± 1.66*
TEL	-1.89 ± 2.51

The viability of cells was measured by determining the cfu present after treatment and normalizing the data so that cells expressing WT *E. coli* MscL were 100% and cells expressing the empty plasmid were 0%. When significant, the results from Student's t test are shown versus the empty plasmid control, (** p < 0.005, * p < 0.05)

Figure 4.2 Channel Kinetics Follow the S1-TM1

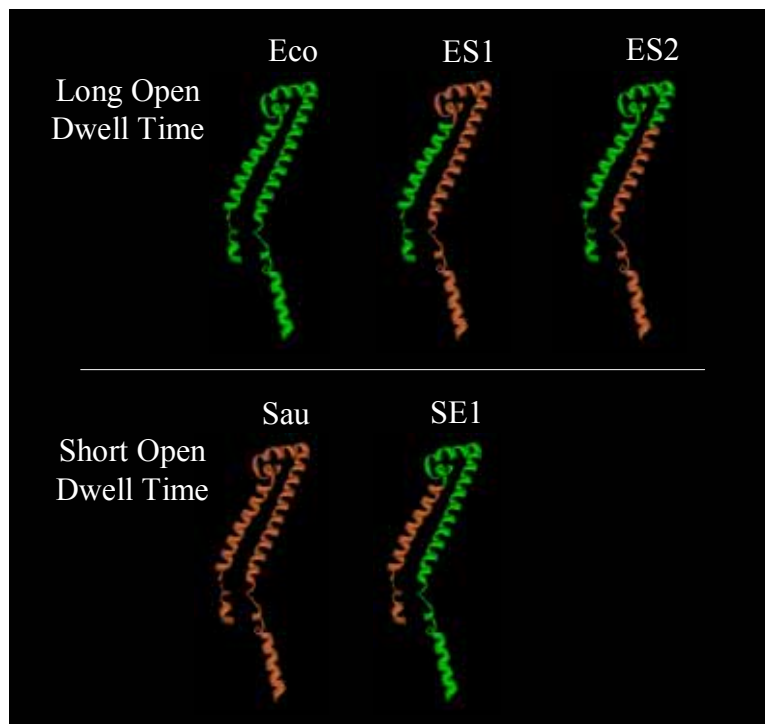


Figure 4.2 A pictorial representation of Eco-Sau chimeras based upon the *E. coli* MscL models is presented. The chimeras are divided according to the kinetics observed during patch clamp studies.

Figure 4.3 Single Channel Traces Illustrating Channel Kinetics

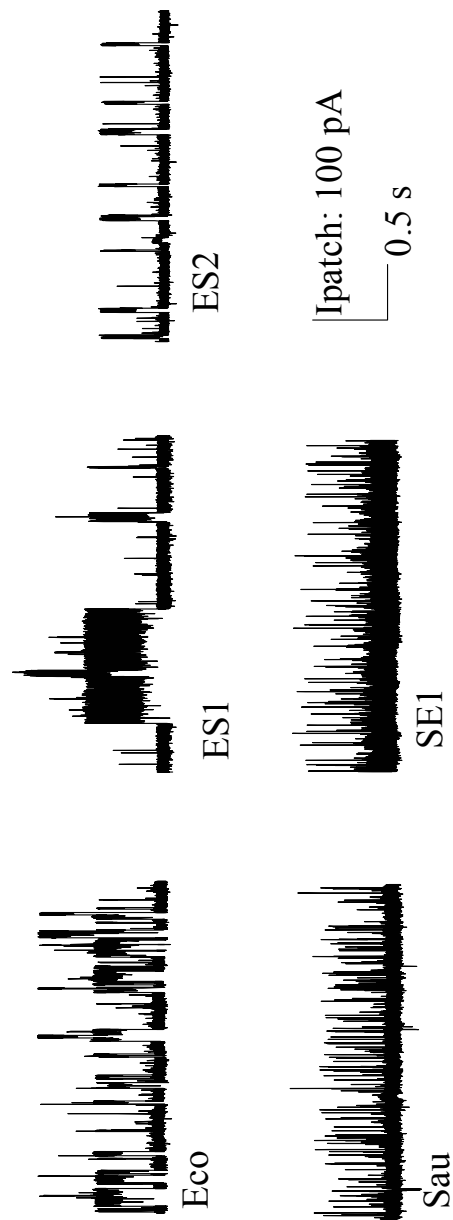


Figure 4.3 Single channel traces of the Eco-Sau chimeras show that the kinetics of the channel follow the parent from which the TM2 was derived.

Table 4.2 Patch and *in vivo* Results for Eco-Sau chimeras

	Normalized % Viability	Tension Sensitivity		Conductance (g) pA	Dwell Time (ms)		
		Threshold MscL/MscS			τ_2	τ_3	
Eco	100.0 \pm 0.0	1.38 \pm 0.05 ‡		83 \pm 2 ‡	4.279 \pm 0.82	15.651 \pm 2.11 ‡	
Sau	84.53 \pm 19.05 †	1.90 \pm 0.11 †		50 \pm 3 †	<1	<1 †	
ES1	152.6 \pm 29.41 ‡	1.65 \pm 0.07 †		68 \pm 3 ‡†	<1	2.216 \pm 0.24 ‡†	
ES2	ND	1.41 \pm 0.14 ‡		67 \pm 2 ‡†	2.916 \pm 0.72	14.855 \pm 1.88 ‡	
SE1	56.14 \pm 7.10 †	1.55 \pm 0.12		73 \pm 4 ‡†	<1	<1 †	
SE2	27.44 \pm 5.92 †	>1.70		ND	ND	ND	

ND – Not determined. ES2 was not examined *in vivo* because it exhibits a gain-of-function phenotype.

SE2 kinetics and conductance could not be determined due to fragility of patch.

τ_1 was <1 in all cases.

† Statistically different from Eco ($P < 0.05$ as determined by Student's t test)

‡ Statistically different from Sau ($P < 0.05$ as determined by Student's t test)

Figure 4.4 Channel Conductance Follows TM2

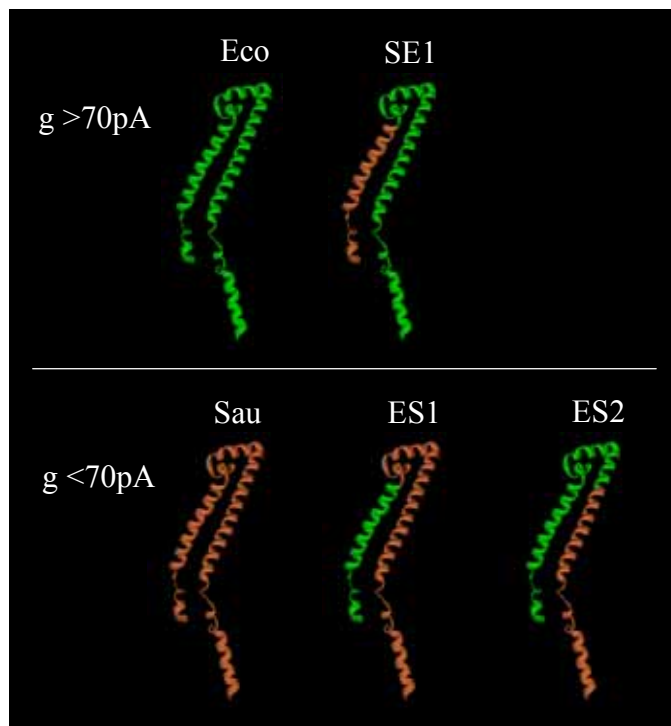


Figure 4.4 A pictorial representation of Eco-Sau chimeras based upon the *E. coli* MscL models is presented. The chimeras are divided according to the conductance observed during patch clamp studies.

Chapter 5 : Materials and Methods

Strains

E. coli strain PB104 ($\Delta mscL::Cm$; Blount, Sukharev et al. 1996), was used to host the pB10b expression constructs (Blount, Sukharev et al. 1996; Ou, Blount et al. 1998; Moe, Levin et al. 2000) for GOF and electrophysiological analysis. Similarly, MJF455 ($\Delta mscL::Cm$, $\Delta mscS$; Levina, Totemeyer et al. 1999), was used as host for the in vivo functional assays. All strains were routinely grown in Lennox Broth (LB) at 37°C, in a shaking-incubator rotated at 250 cycles/min, and retention of the plasmid was ensured by the addition of 1mM ampicillin. Furthermore, only recently streaked colonies (plates removed from the incubator within the past 48 hours) were used for starting cultures. This was necessary since some of the channel mutations caused growth defects in the cell and after 48 hours revertants, changes in the plasmid, or compensatory mutations could arise in the cell. The wild-type *E. coli mscL*, *M. tuberculosis mscL*, *S. aureus mscL*, *Synechocystis* PCC6803 *mscL*, *B. subtilis mscL*, chimeric *mscL* mutants, and cysteine substituted *mscL* mutants were inserted into the plasmid pB10b and expression was induced using isopropyl β -D-thiogalactoside (IPTG). The cysteine mutant library was generated by Dr. Gal Levin as described below and published previously (Levin and Blount 2004). Construction of chimeras is described below.

Construction of cysteine mutants

The cysteine library was constructed and characterized by Dr. Gal Levin previously (Levin and Blount 2004). Briefly, the mutants were constructed through polymerase chain reaction, using either a QuikChange site-directed mutagenesis kit (Stratagene, La Jolla, CA) or a modified megaprimer protocol. The megaprimer protocol consisted of two separate reactions using the wild-type gene on a plasmid as the template; the first reaction utilized an internal primer that contained the desired mutation and a complementary external primer that created a fragment of the gene including the mutation (termed the megaprimer). The secondary reaction combined the megaprimer created in the first reaction with another external primer in order to amplify the complete gene while maintaining the point mutation. The full-length product was ligated into pBluescript and sequenced in both directions to verify the single mutation. The mutated *mscL* was then subcloned into the pB10b expression vector utilizing either of the set of restriction enzyme consensus site pairs XbaI/SalI or XbaI/XhoI (Blount, Sukharev et al. 1996; Blount, Sukharev et al. 1996). The codon used for cysteine was TGC except for G22C, a generous gift from Professor Ching Kung (University of Wisconsin, Madison), which used TGT.

Construction of chimeras

The chimeras were constructed using a multi-round PCR (**Figure 5.1**). Expand High Fidelity was used according to the manufacturer's instructions (Roche). In the primary reaction, the appropriate external 5' primer and internal 3' primer were used to amplify the beginning portion of the chimera (**Table 5.1 and 5.2**). Since only a portion of the internal primer matched the template, five rounds were completed of melting at 94°C for 1min, annealing at 50°C for 1min, and extension at 72°C for 1.16min. Then, in order to preferentially amplify the desired fragment, the same cycle was repeated 25 times but with an annealing temperature of 65°-72°C, depending on the primer. At the same time, the appropriate internal 5' primer and external 3' primer were used to amplify the other portion of the chimera using the same cycle times and temperatures. In the case of Eco-Tb chimeras, T7 and T3 were used for the external 5' and 3' primers, respectively. For the Eco-Sau chimeras, the EcomscL 5', EcomscL3', SaLink5', and SaLink 3' primers were used for the external primers (see **Table 5.1 and 5.2**). The internal 5' and 3' primers were named for the chimera they produced and overlap each other in sequence as well as covering the entire junction between the two *mscL* sequences being grafted (**Figure 5.1 and Table 5.1**). In the secondary reaction of PCR, the two portions of *mscL* produced in the primary reactions were allowed to prime each other and external primers were used to amplify the complete sequence. The resulting chimeric *mscL* was ligated into a cloning vector

(topo) and transferred into TOP 10 cells using the Zero Blunt TOPO PCR Cloning Kit for Sequencing version H according to the manufacturer's instructions (Invitrogen). The resulting vector was purified and the insert sequenced in both directions to confirm the composition of the chimera. The chimera gene was then excised using convenient restriction enzyme sites and ligated into the vector pB10b. The sequence was once again confirmed by sequencing.

***In vivo* gain of function assay**

A recently streaked, single colony of PB104, expressing the gene of interest, was grown overnight at 37°C in LB plus 1mM ampicillin. PB104 was used because it is lacking *mscL*, but all of the other mechanosensitive channels are present. Therefore, the growth phenotype monitored should be due to the presence of the mutant MscL alone. Cells expressing the empty vector and Eco *mscL* were grown at the same time and in the same manner as controls. In the case of chimera mutants, cells producing the Tb and Sau MscL channels were also grown as controls. The overnight culture was diluted into two flasks at a dilution of 1:100 into 10ml of LB + 1mM ampicillin. The cultures were grown and the OD₆₀₀ measured roughly every 20-30 minutes. When cultures reached an OD₆₀₀ near 0.1, 1mM IPTG was added to one flask of each culture in order to induce expression of the plasmid. The OD₆₀₀ was then measured until the cultures reached stationary phase. The resulting OD's were graphed versus time in order to obtain a growth

curve for the different mutants. If an induced cell line had a slower growth rate or entered stationary phase early compared to the uninduced culture, then it was termed a gain-of-function mutant.

***In vivo* functional assay performed on chimera mutants**

Recently streaked colonies of MJF455 expressing the gene of interest were grown overnight at 37°C in 1mL of citrate-phosphate defined medium (per liter: 8.57g Na₂HPO₄, 0.87g K₂HPO₄, 1.34g citric acid, 1.0g NH₄SO₄, 0.001g thiamine, 0.1g Mg₂SO₄·7H₂O, 0.002g (NH₄)₂SO₄·FeSO₄·6H₂O) plus 1mM ampicillin and 0.04% glucose. MJF455 was chosen due to its lack of both *mscL* as well as *mscS*. MscS, therefore, could not compensate for a malfunctioning MscL channel. The cells were grown overnight in low glucose in order to limit the growth and arrest the cells in the same phase of the cell cycle. The overnight cultures were supplemented in the morning with glucose to 0.2% glucose and grown for 1hr. The cultures were then diluted to an OD₆₀₀ of 0.05 in 3ml of the citrate-phosphate media with 0.2% glucose. This allowed the cells to fully recover from any modifications they may have made in stationary phase before exposure to the hyperosmotic stress. After growing to an OD₆₀₀ 0.1, the cultures were mixed 1:1 volume with citrate-phosphate media containing 0.2% glucose and 1M NaCl thereby bringing the final salt concentration to 0.5M. They were then grown to an OD₆₀₀ of 0.2-0.25 at which stage expression was induced for 1 hour with 1mM

IPTG. The induced cultures were diluted 1:20 into citrate-phosphate medium containing 0.5M NaCl as a mock shock or ddH₂O for hypo-osmotic shock. Cells were grown with shaking at 37°C for 15 min. and then six consecutive 1:10 serial dilutions were made in citrate-phosphate medium containing 0.2% glucose and 0.5M NaCl. These diluted cultures were plated in duplicate and grown overnight at 37°C on LB-ampicillin agar plates. The colony forming units (cfu) were counted from plates that contained 40-400 colonies in order to minimize error, and the duplicate plates were averaged per experiment. The cfu's were then converted to a percentage viability compared to the mock-shock (control) condition. Mean \pm SEM for all values are shown and statistically significant differences were determined by a Student's t test. Below is a detailed protocol modified from a laboratory procedure.

Citrate-Phosphate Defined Media Logarithmic LOF 96-well plate

1. Inoculate overnight culture from single colony into 2ml cit-phos media, low glucose (0.04%), supplements, and amp (see o/n solution below). Do this before 1pm but not before 11am.
2. In the morning read OD₆₀₀
3. Supplement glucose. (20ul/tube) Grow 1 doubling ~1hr.

4. Measure OD
5. Sub cultures into normal glucose cit-phos media. Make the final concentration \sim OD= 0.5 in 3ml.
6. Grow 1hr or to OD \sim 0.1. Measure OD.
7. Sub into high salt cit-phos media. 2:1 in 2ml (So high salt solution should be 1M for a final concentration 0.5M)
8. Grow about 3.5hr to OD \sim 0.2
9. Add IPTG and grow for 1hr. Prepare 96 well plate for shocking and dilution.
10. Measure OD
11. Shock 2ul of culture in 198ul of dH₂O. Dilute unshocked control in high salt media. 30 minutes room temperature.
12. Make first dilution in same order of shocking (20ul in 180ul 1X salt media).
13. Use multi-channel to make rest of dilutions.
14. Drop Plates using 5ul onto no line square LB plates.

<u>O/N solution</u>	<u>Step 5</u>	<u>Step 7</u>	<u>Step 9</u>
200ul Mg ₂ SO ₄	300ul Mg ₂ SO ₄	2.4ml NaCl	1.2ml NaCl
200ul Thiamine	300ul Thiamine	400ul Mg ₂ SO ₄	200ul Mg ₂ SO ₄
200ul Iron	300ul Iron	400ul Thiamine	200ul Thiamine
40ul glucose	300ul glucose	400ul Iron	200ul Iron
20ul amp	27ml Water	400ul glucose	200ul glucose
18ml Water	3ml 10X cit-phos	33.6ml Water	16.8ml Water
2ml 10X cit-phos	media	4ml 10x cit-phos	2ml 10X cit-phos

Stocks: 40mM MgSO_4 , 0.3 mM Thiamine-HCl, 20% glucose, 100ug/ml Amp, 0.6mM $(\text{NH}_4)\text{FeSO}_4$, 500 ml of 10X cit-phos (42.9 g Na_2HPO_4 , 4.35g K_2HPO_4 , 6.7g citric acid, 5.0g NH_4SO_4)

***In vivo* functional assay performed on cysteine mutants**

Recently streaked colonies were grown overnight at 37°C in 1mL of citrate-phosphate defined medium (per liter: 8.57g Na_2HPO_4 , 0.87g K_2HPO_4 , 1.34g citric acid, 1.0g NH_4SO_4 , 0.001g thiamine, 0.1g $\text{Mg}_2\text{SO}_4 \cdot 7\text{H}_2\text{O}$, 0.002g $(\text{NH}_4)_2\text{SO}_4 \cdot \text{FeSO}_4 \cdot 6\text{H}_2\text{O}$) plus 1mM ampicillin and 0.2% glucose. MJF455 was chosen due to its lack of both *mscL* and *mscS*. MscS, therefore, could not compensate for a malfunctioning MscL channel. The fresh overnight culture was diluted 1:20 in 2ml of this defined medium and grown for 1 hr. This allowed the cells to fully recover from any modifications they may have made in stationary phase before exposure to the hyperosmotic stress. The culture was then diluted to an OD_{600} 0.05 in 2ml of the same medium and supplemented with 0.5M NaCl. The cultures were grown to an OD_{600} of 0.2-0.25 at which stage expression was induced for 1 hour with 1mM IPTG. The induced cultures were diluted 1:20 into citrate-phosphate medium containing: 1) 0.5M NaCl as control; 2) no additives for hypo-osmotic shock; 3) 0.5M NaCl and 1mM MTSET for MTSET alone; or 4) 1mM MTSET for MTSET and hypo-osmotic shock. The primary screen

utilized only the first and fourth condition while all four were tested in subsequent experiments. MTSET was chosen because it is a small, positively charged sulfhydryl reagent and should therefore only react with residues aqueously exposed. It has been reported to have a short half-life in water, so the MTSET powder was kept cold and the mixture was made immediately before use. Cells remained at room temperature in media for 30 minutes and then six consecutive 1:10 serial dilutions were made in citrate-phosphate medium containing either no salt (for the hypo-osmotic shock conditions) or 0.5M NaCl (for the mock-shock conditions). These diluted cultures were plated in duplicate and grown overnight at 37°C on LB-ampicillin agar plates. The colony forming units were counted from plates with 40-400 colonies and the duplicates averaged per experiment. All data are presented as a percentage of the mock-shock (control) condition. Mean \pm SEM for all values are shown and statistically significant differences were determined by a Student's t test. [2-(trimethylammonium) ethyl]methanethiosulfonate bromide (MTSET) was obtained from Toronto Research Chemicals, Ontario, Canada. Below is a detailed protocol modified from a laboratory procedure.

***In vivo* Cysteine Assay Citrate-Phosphate Defined Media**

1. Night before inoculate 2mL Citrate phosphate defined media pH 7.0 (CPhM) normal glucose and 100ug/mL Amp and grow overnight.
2. Dilute 100uL of overnight culture into 2mL of CPhM.
3. Grow at 37°C to an OD₆₀₀ 0.5-1.2.
4. Dilute to an OD₆₀₀ 0.05 into 2mL of pre-warmed CPhM with 0.5 M NaCl (add 286ul of 4M NaCl to already diluted culture).
5. Grow to an OD₆₀₀ ~0.25 and induce with 1mM IPTG.
6. Grow for 1 hour at 37°C. Read OD.
7. Dilute cultures 1:20 into shocked and unshocked (50μL into 1mL).
8. Shake at 37°C for 15 minutes.
9. Make ten-fold dilutions of shocked cells into high- or no-salt media in a 96-well plate (20μL into 180μL).
10. Plate onto LB Amp plates and grow overnight at 37°C.
11. Count CFU's.

Shock Media: CPhM pH 7.0 with 1.0mM MTSET (or other sulfhydryl reagent)

Unshocked: CPhM pH 7.0 with 0.5 M NaCl and 1.0mM MTSET (or other sulfhydryl reagent)

Shock Procedure: Set up small tubes with 940 μ L of media w/o MTSET and pre-warm. Tubes of MTSET in freezer make 250 μ L of 100x MTSET (100mM).

Immediately before shocking make up 100x MTSET with sterile water and add 10 μ L to each tube. Then add 50 μ L of cells and shake for 15 minutes.

<u>CPhM (40ml)</u>	<u>CPhM High Salt (32ml)</u>
400ul Mg ₂ SO ₄	320ul Mg ₂ SO ₄
400ul Thiamine	320ul Thiamine
400ul Iron	320ul Iron
400ul glucose	320ul glucose
40ul amp	4ml 4M NaCl
36ml Water	32ul amp
4ml 10X cit-phos media	24.8ml Water
	3.2ml 10X cit-phos media

Stocks: 40mM MgSO₄, 0.3 mM Thiamine-HCl, 20% glucose, 100ug/ml Amp, 0.6mM (NH₄)FeSO₄, 500 ml of 10X cit-phos (42.9 g Na₂HPO₄, 4.35g K₂HPO₄, 6.7g citric acid, 5.0g NH₄SO₄)

Spheroplast Preparation

E. coli giant spheroplasts were generated as described previously (Martinac, Buechner et al. 1987). Briefly, a PB104 culture expressing the gene of interest was grown overnight in LB plus 1mM ampicillin. The PB104 cell line was chosen because it produces MscS, which we use as an internal control in the patching analysis of MscL (described below). After overnight growth, the culture was diluted 1:100 into 10ml of LB media and allowed to grow to an OD₆₀₀

0.1~0.2. This procedure allowed the cell to recover from changes made during stationary phase in the night. Then the culture was diluted 1:10 in a total of 30ml of media with 60ug/ml of cephalixin. This procedure allowed the cells to continue growing, but prevented them from undergoing septation, thereby forming long filamentous cells (see **Figure 5.2**). Cells were allowed to grow until the filamentous cells were roughly 50-150 um. During the last 5-15 minutes of growth in cephalixin, expression of the plasmid was induced with 1mM IPTG. If the mutant caused a severe GOF phenotype, then the induction was sometimes eliminated because the cells could become extremely fragile and fail to form spheroplasts. As previously established, even without induction a few channels are still expressed (Blount, Sukharev et al. 1999). The filamentous cells were harvested by centrifugation at 1500 rpm for 5 minutes and the supernatant was aspirated. 2.5ml of 0.8M sucrose was then used to gently resuspend the filamentous cells without pipetting. The following reagents were added in order: 125ul of 1 M Tris Cl (pH 8); 120ul of lysozyme (5 mg/ml); 30ul of DNase 1 (5 mg/ml); 150ul of 0.125M Na EDTA (pH 7.8). This treatment hydrolyzed the peptidoglycan layer and nicked up the outer membrane. The mixture was allowed to react for 5 minutes at room temperature and then stopped using 1ml of an ice cold solution containing 0.7M sucrose, 20mM MgCl₂, and 10mM Tris Cl. This step removes the EDTA and activates the DNase. The mixture was then layered over two 13 x 100mm culture tubes containing 7ml of an ice cold solution

composed of 0.8 M sucrose, 10mM MgCl_2 , and 10mM Tris Cl (pH 8). The spheroplasts were harvested by centrifugation of the tubes at 4°C for 2 minutes at 1500rpm. All but roughly 300 μl of the supernatant was removed and the pellet resuspended in the remaining liquid. The spheroplasts were aliquoted and stored long term at -20C. Aliquots were kept on ice during the day they were used in an experiment and normally thrown away after that day. Frozen preparations were usually used within a week. There was no change in channel activity between fresh and frozen or refrozen preparations, but over time the fragility of the membrane seemed to increase which made obtaining high pressures difficult. Below is a detailed protocol, with many lab members contributing to the final arrangement.

***E. coli* Giant Spheroplast Preparation**

Stocks

- Na•EDTA 125mM pH 7.8
- Tris•Cl 1M pH 8.0
- MgCl₂ 1M
- Sucrose 0.8M 4°C
- Cephalixin 10mg/ml
- Lysozyme 5mg/ml
- DNAase 5mg/ml
- IPTG 1M

Solutions

Stop solution (1ml per prep)

- 875µl 0.8M sucrose
- 95µl ddH₂O
- 20µl 1M MgCl₂
- 10µl 1M Tris•Cl

Dilution Solution (15ml per prep)

- 15ml 0.8M sucrose
- 150µl 1M MgCl₂
- 150µl 1M Tris•Cl

1. Grow overnight culture in LB amp (1ml).
2. Subculture O/N 1:100 to 10ml LB amp. Shake, 37°C to OD₆₀₀ 0.1 ~0.2.
3. Subculture 3ml into 27ml LB amp. Add 180µl Cephalixin, grow until filamentous cells are long enough (~2hrs no more than 3hrs). Then, if adding IPTG, add 50µl and grow 10min.
4. Harvest 1500 rpm 10min, 50ml conical tubes. Aspirate supernatant.
5. **Gently** resuspend in 2.5ml 0.8M sucrose and do reaction 5 min. (NO pipetting) If obtaining spheroplast is difficult for a mutant, follow reaction on scope and stop when appropriate.

<u>Reaction</u>	
To each tube add in order: <ul style="list-style-type: none"> • 125µl Tris•Cl • 120µl lysozyme • 30µl DNAase • 150µl EDTA 	Begin timer at Tris addition, Swirl tubes after each step. 2 samples- lysozyme 1.5mg/300ul, DNase 0.5mg/100ul.

5. Add 1ml Stop solution to stop reaction, mix **gently** and immerse in ice.
6. Harvest spheroplasts through sucrose gradient:

 Carefully layer ½ reaction per top of 7ml 0.8M sucrose in 10ml glass tubes. (2 per prep). Spin 1500rpm, 2min. If necessary, repeat with speed increased in 250 rpm increments to 2000rpm max. The pellet is usually small and difficult to see.
7. Remove supernatant, leaving ~300µl per tube. Resuspend **gently**, and aliquot to 50µl fractions. Store at -20°C. Preps are good up to 1 month at -20°C.

Electrophysiology

E. coli giant spheroplasts were generated as above and used in patch-clamp experiments as described previously (Blount and Moe 1999). Basically, 1-5µl of the spheroplast solution was placed in a recording bath containing a buffer comprised of 200mM KCl, 90mM MgCl₂, 10mM CaCl₂, and 5mM HEPES adjusted to pH 6.0. Patch pipettes were pulled (discussed below) and filled with the same buffer as the recording bath, except in the backfill experiments where the tip of the pipette was filled with the recording solution and the rest of the

pipette was filled with the same solution containing MTSET. As in the *in vivo* experiments, due to its short half-life, MTSET was stored in aliquots in the cold as a powder and only mixed with liquid right before its use. The solution was then only used within the first 10 minutes. For experiments utilizing MTSET, 1mM final concentration was added to the bath after seal formation for cytoplasmic exposure and 2mM was added in backfill to the pipette for periplasmic exposure. Patches were formed by inserting the pipette into the bath and applying a slight negative pressure in order to draw the spheroplast toward and up into the tip of the pipette (see **Figure 5.2**). In this manner, a patch of membrane was pulled up into the pipette with the cytoplasmic side of the bilayer facing the bath, called an inside-out patch. Stable patches (those that formed gigaohm seals) were excised from the remaining membrane by the application of a slight tap on the microscope stage. All experiments were conducted at room temperature and spheroplasts were chosen based on their appearance. Symmetrically round, light reflecting ‘shiny’ spheroplasts by phase microscopy usually yielded the most stable patches. However, some GOF mutants mainly produce very dark or ghost-like spheroplasts; in this case, patches from the dark spheroplasts tend to yield more channels than the shiny spheroplasts, presumably because the channels were destabilizing the spheroplast. Once stable, excised patches were obtained, recordings were performed while holding the voltage at -20 mV and varying the pressure across the membrane. Conductance data were acquired at a sampling rate

of 50 kHz with a 10 kHz filter using an AxoPatch 200B amplifier in conjunction with Axoscope software (Axon Instruments, Union City, CA). A piezoelectric pressure transducer (World Precision Instruments, Sarasota, FL) was used to measure the pressure throughout the experiments.

Patch pipettes were pulled from borosilicate capillary tubes (100ul Disposable Microliter Pipets, Fisher brand) to tip diameters of 0.08-0.2 μm using a Flaming/Brown Micropipette Puller. Basically, a current is passed through a metal filament which melts the glass capillary tube and pressure applied to both sides of the glass pulls it thin until the capillary separates into two pipettes with large diameter tips. A program is used that consists of one or more cycles which, when executed in sequence, will 'pull' the capillary glass inserted in the instrument. A cycle consists of four programmable parameters; heat (the level of electric current applied to the filament which melts the glass), pull (the amount of final pull applied to the glass, changes the taper), velocity (measured as the glass softens and begins to pull apart under constant load, when value is reached the heat turns off and cooling air starts), and time or delay (time of cooling air on filament in-between cycles). In addition, a blast of air cools the filament after the heating segment of a pull cycle, based on the type of glass used we followed the manufactures recommendation of 500 units (Operations Manual). The heat is determined based on the composition of the glass to be pulled and characteristics of the heating filament. A ramp test is used to establish an optimal heat value as a

function of the filament/glass combination. Basically, the glass is pulled with the heat of the filament increased at a rate of 650milliamps/sec until the factory set velocity is reached. This determined ramp value is then the suggested starting value for heat during the cycles and can be increased by up to 30-35 units in order to change the length and tip size of the pipette. Four cycles were used. The first with a heat=269, pull=0, velocity=40, delay=150. The second with a heat=254, pull=0, velocity=40, delay=150. The third with a heat=218, pull=0, velocity=40, delay=150. The fourth with a heat=272, pull=45, velocity=50, delay=5. The pipette tip size was tested before and after a series of pipettes were pulled in order to confirm that the tip size is relatively constant. This procedure was accomplished by determining the “bubble number” (Corey and Stevens 1983). The pipette was attached to a 10ml syringe via an air-tight piece of tubing that was already filled with room air. The tip of the pipette was submerged in methanol and the minimum pressure was applied to the syringe until the surface tension was overcome at the tip and a stream of bubbles was expelled. The volume (in milliliters) to which the air must be compressed before bubbles escape from the tip is the bubble number. The higher the number, the larger the pipettes tip.

Analysis

The mechanosensitive channels open in response to tension within the membrane, but it is difficult to visualize the patch and determine the tension within the membrane on a regular basis. Therefore, we applied and measured pressure across the membrane and reported the required amount of stimuli necessary to open the channel as tension sensitivity, using MscS as an internal control. The tension sensitivity was determined by dividing the MscL pressure threshold with that of MscS, as previously described (Blount, Sukharev et al. 1996; Blount and Moe 1999; Ou, Blount et al. 1998), since the ratio between MscL and MscS from the same patch is relatively uniform across preparations. MscS threshold was determined as the pressure needed, within 7 sec, to open two or more channels as evidenced by two-storied events. The MscL threshold was defined as the pressure at which openings were readily observed every 0.5 to 2 sec (Blount, Sukharev et al. 1996). A minimum of three patches from different preparations were used in all analyses and the SEM reported in every calculation. Conductance of the channel was measured both by manually calculating channel conductance as well as by plotting an all-points histogram (using PCLAMP 8.1) in which the population of both sub-states and fully open states could be seen. When choosing traces for analysis, only those exhibiting almost exclusively one channel opening were used, otherwise the dwell-time analysis could have been skewed, because if two or more channels are open in the trace at the same time

and one closes, there is no way to tell which of the channels closed, thereby complicating analysis. The dwell times were calculated from these single opening traces using the software from PCLAMP version 8.1 (Axon Instruments, Union City, CA). Dwell times of less than 1ms are below the resolution of the equipment and therefore reported as <1ms. Open dwell times were fit to a three-open state model; τ_2 and τ_3 are the two longer time constants. The shortest τ for each group, which was always <1ms, could not be measured accurately and was not shown. Mean \pm SEM for all values are shown and statistically significant differences were determined by a Student's t test.

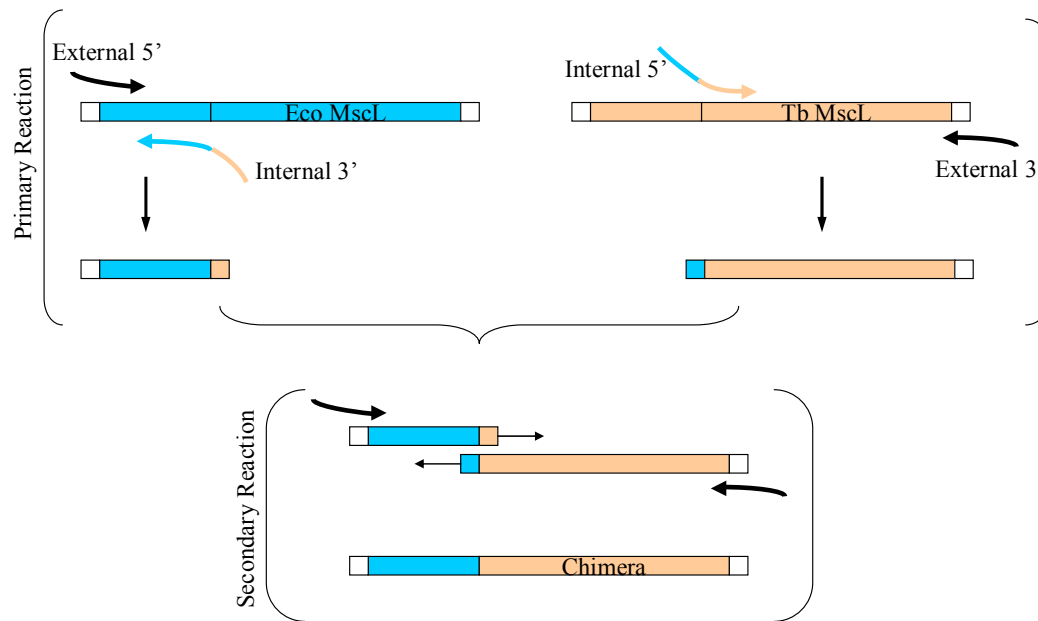
Figure 5.1 Multi-round PCR Used to Construct *mscL* Chimeras

Figure 5.1 In the primary round of PCR, two DNA fragments were amplified in separate PCRs using an internal primer specific to the final sequence desired and an external primer specific to the parental DNA. This created two halves of the final chimera. In the secondary reaction, the two PCR products were then mixed, denatured, reannealed, and used as templates for a further round of PCR using the external primers. The products were then cloned into TOPO and the sequence confirmed by DNA sequencing.

Figure 5.2 Visualization of a Patch

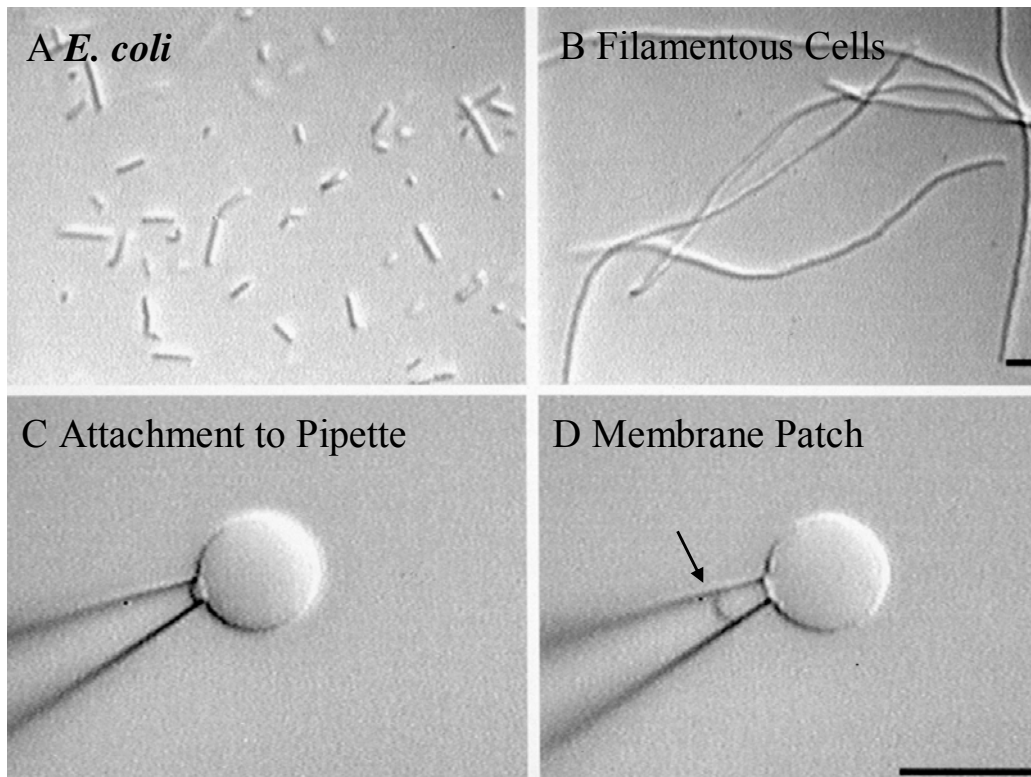


Figure 5.2 The first panel (A) shows a picture of normal *E. coli* cells. (B) The cells are grown in cephalixin, which inhibits septation, and they form long filamentous cells. (C) After exposure to lysozyme and EDTA, the snakes become large spheroplasts, consisting mainly of the inner membrane. A glass pipette is shown next to the spheroplast. (D) Positive suction applied draws a patch of the membrane up into the pipette, indicated by the arrow. The bar represents 10 μ m.

Table 5.1 Sequences of Primers Used to Make Chimeras

Primer Name	Sequence
T3+	AAT TAA CCC TCA CTA AAG GGA ACA AAA
T7+	TAA TAC GAC TCA CTA TAG GGC GAA TTG G
EcoTb1 5'	GTT GCC GAT ATC ATT ACG CCG CTG ATC AAC C
EcoTb1 3'	CAG CGG CGT AAT GAT ATC GGC AAC CAG TGA A
EcoTb2 5'	GAT GCA TTA CGG TGT CTT GTT GTC GGC AGC G
EcoTb2 3'	CGA CAA CAA GAC ACC GTA ATG CAT CAC AAC AG
TbEco1 5'	CCG ACA GCA TCA TCA TGC CTC CTC TGG GCT
TbEco1 3'	AGG AGG CAT GAT GAT GCT GTC GGT GAA CTT G
TbEco2 5'	CAT TGA CTT GAA CGT CTT CAT TCA AAA CGT CTT TG
TbEco2 3'	TTT TGA ATG AAG ACG TTC AAG TCA ATG GTC TGA CC
ETF29 5'	ATC GGT GCG GCA TTC ACG GCG TTG GTC ACC A
ETF29 3'	CAA CGC CGT GAA TGC CGC ACC GAT AAT GA
TEF29 5'	ATC GGC ACA GCG TTC GGG AAG ATT GTC TCT TCA
TEF29 3'	AAT CTT CCC GAA CGC TGT GCC GAT TAC C
EcomseL5'	TCT AGA TCT AGA CTT ATG GTT GTC GGC TT
EcomseL3'	CTC GAG CTC GAG CTT GTT AAG AGC GGT TAT TC
Saulink5'	TCT AGA TCT AGA GTT ACA TTT AAA AAA GAG AG
Saulink 3'	TAC CGG TAC CGC CTC GAG CTT TTT ATT TAA AAA
EcoSau1 5'	ATC ATC ATG CCA TTA ATT GGT AAA ATT TTC GGA TCA
EcoSau1 3'	ACC AAT TAA TGG CAT GAT GAT ATC GGC AAC CAG
EcoSau2 5'	GTG ATG CAT TAC GGT TTA TTT ATC CAA TCT GTT
EcoSau2 3'	TTG GAT AAA TAA ACC GTA ATG CAT CAC AAC AGC
SauEco1 5'	GAA AAT ATC ATT ATG CCT CCT CTG GGC TTA TTA
SauEco1 3'	GCC CAG AGG AGG CAT AAT GAT ATT TTC TAC TAA
SauEco2 5'	GGT ATT AAA TAC GGT GTC TTC ATT CAA AAC
SauEco2 3'	AAT GAA GAC ACC GTA TTT AAT ACC CCA GAA

Table 5.2 Position of Chimera Junction in Protein and Primers Used

Chimera	Junction Position in Protein	Primers used in Primary rxn. (Template)	Primers used in Secondary rxn.
ET1	Eco 40 Tb 39 (I-I)	EcomscL5' and EcoTb1 3' (Eco); EcoTb1 5' and T3+ (Tb)	T7+ and T3+
ET2	Eco 77 Tb 72 (N-V)	EcomscL5' and EcoTb2 3' (Eco); EcoTb2 5' and T3+ (Tb)	T7+ and T3+
TE1	Eco 41 Tb 38 (I-I)	T7+ and TbEco1 3' (Tb); TbEco1 5' and EcomscL3' (Eco)	T7+ and T3+
TE2	Eco 78 Tb 71 (N-V)	T7+ and TbEco2 3' (Tb); TbEco2 5' and EcomscL3' (Eco)	T7+ and T3+
E29T	Eco 28 Tb 27 (A-F)	T7+ and ETF29 3' (Eco); ETF295' and T3+ (Tb)	T7+ and T3+
T29E40	L: Tb 26 Eco 29 (A-F) R: Eco 40 Tb 39 (I-I)	T7+ and TEF29 3' (Tb); TEF29 5' and T3+ (ET1)	T7+ and T3+
ETL	L: Eco 40 Tb 39 (I-I) R: Tb 71 Eco 78 (N-V)	T7+ and EcoTb1 3' (Eco); EcoTb1 5' and EcomscL 3' (TE2)	T7+ and T3+
TEL	L: Tb 38 Eco 41 (I-I) R: Eco 77 Tb 72 (N-V)	T7+ and TbEco1 3' (Tb); TbEco1 5' and EcomscL 3' (ET2)	T7+ and T3+
ES1	Eco 40 Sau 39 (I-I)	EcomscL5' and EcoSau 1 3' (Eco); EcoSau1 5' and Saulink 5' (Sau)	SaLink5', and SaLink 3'
ES2	Eco 77 Sau 64 (Y-G)	EcomscL5' and EcoSau2 3' (Eco); EcoSau2 5' and Saulink 5' (Sau)	SaLink5', and SaLink 3'
SE1	Eco 41 Sau 38 (I-I)	Saulink 5' and SauEco1 3' (Sau); SauEco1 5' and EcomscL 3' (Eco)	SaLink5', and SaLink 3'
SE2	Eco 78 Sau 63 (Y-G)	Saulink 5' and SauEco2 3' (Sau); SauEco2 5' and EcomscL 3' (Eco)	SaLink5', and SaLink 3'

The specific junction in the protein is listed for each chimera. In the first column is the name of the chimera. In the second column, the contributing parents are listed linearly in the order that they contribute to the sequence, followed by the last or first residue number retained from that particular channel (so the residue number used is from the parental sequence). In parenthesis are the single letter codes of the amino acids that the residue number corresponds to. Because only conserved junctions were chosen, the amino acids are the same for both parental sequences. Where two junctions are present, they are delineated by L for left and R for right where the sequence begins on the left with the N-term. For example, ET1 begins with the E. coli N-term and goes through residue I40. The rest of the sequence comes from the M. tuberculosis channel starting with the I39 residue in its sequence. In the third and fourth columns are the primers used to create each chimera with the template used in parenthesis.

Chapter 6 : Discussion

The mechanosensitive channel of large conductance acts as an ‘emergency release valve’ in bacteria by sensing tension in the membrane and converting that energy into channel gating (Levina, Totemeyer et al. 1999). While this channel has been studied for many years, the structural transitions that occur upon gating have been questioned. Previous mutagenic studies have demonstrated that more charged or hydrophilic mutations in or around the pore can lead to a change in channel gating (Ou, Blount et al. 1998; Yoshimura, Batiza et al. 1999; Maurer and Dougherty 2001), which often results in a phenotypic change within the cell (Ou, Blount et al. 1998). In this work we capitalize on the ability to change channel gating and phenotypes in order to elucidate movements within the channel and specify residues that might be involved in sensation and gating.

The first strategy utilized was a modified *in vivo* SCAM. Sulfhydryl reagents, including methanethiosulfonate compounds (MTS), have been used in the past to probe the pore of several other channels (Akabas and Karlin 1999), indicating which residues are exposed and often changing the conductance. However, the conductance of MscL has never been altered by the addition of MTS reagents (Yoshimura, Batiza et al. 2001; Batiza, Kuo et al. 2002; Chapters 2 and 3), probably due to the very large pore estimated at about 30Å (Cruickshank,

Minchin et al. 1997). Since electrophysiological characterization of charged mutants demonstrated a correlation between the severity of the slow- or no-growth phenotype, a leftward-shift of the activation curve (the mutant channels were more sensitive to stimulus) and a decrease in the open dwell time of the channel (Ou, Blount et al. 1998), it was postulated that modification of the channel with a charged molecule could be monitored by testing channel function within the cell. This change in *in vivo* function upon post-translational modification was demonstrated by Batiza *et al.* who used the positively charged MTSET to modify MscL channels containing a L19C mutation (Batiza, Kuo et al. 2002). While multiple cell lines were used in that study, we specifically used a *mscL* and *mscS* double-null strain, MJF 455 (Levina, Totemeyer et al. 1999), in order to avoid false-negative results due to MscS function within the cell.

While our initial scan of a transmembrane cysteine library does not distinguish between mutated residues that are modified by MTSET and those conferring constitutive LOF phenotypes, it was quite easy to subsequently identify the residues exhibiting LOF phenotypes. Furthermore we are fairly certain that the decreased viability is not due to MTSET binding in the closed state and causing the channel to be unable to function because residues in group III_a (Table 2.1) show a phenotype independent of shock and residues in group III_b (Table 2.1) gave consistent results when performed in PB104 (Blount, Sukharev

et al. 1996; Ou, Blount et al. 1998), a MscS-containing strain (Batiza, Kuo et al. 2002; data not shown). The cysteine library used here has been previously characterized (Levin and Blount 2004), and the mutants we identify as LOF are consistent with that study. The mutants not identified here are probably not isolated because of slight differences in the osmotic downshock procedure. In addition, we categorize G76C and I92C as LOF; these mutants were not assayed in the previous study because of their GOF phenotype (leaking channels), which produces an additional stress on the cell. Another GOF mutant isolated here, R13C, had the very unique property of actually being saved by the addition of MTSET. More than likely the channel function is restored due to the reestablishment of a charge at this position, which might imply that electrostatic repulsions are necessary in this region for proper gating.

The results obtained from the *in vivo* SCAM as well as the subsequent electrophysiological characterizations give us a new resolution of the pore domain and its transition from the closed to open state. Several residues reacted with MTSET independent of osmotic downshock and elicited a loss of viability phenotype (Chapter 2 group II). These residues reside within the more periplasmic portion of TM1 (**Figure 2.2**) and are thought to form the vestibule of the channel. When modeled onto the crystal structure of the *M. tuberculosis* MscL channel (Chang, Spencer et al. 1998), the residues appear to line one face of the

helix (**Figure 2.3**), however, they do not directly face the lumen but are rotated several degrees clockwise as viewed from the periplasm. When the MscL channel was originally crystallized, the authors noted that it appeared to be in a closed or "nearly closed" state (Chang, Spencer et al. 1998). Models were constructed based on the idea that the crystal structure was fully closed. Recently, however, it has been proposed that the current structural models, including the crystal structure, reflect a "nearly closed" state and that a slight counterclockwise rotation of TM1 is necessary to achieve the native closed state (Levin and Blount 2004). This theory has been supported not only by the G26C disulfide bridging (Levin and Blount 2004), but also by a metal binding study that indicates the G26 residues are positioned in such a way that they, and not V23 as originally proposed, should be the constriction point (Iscla, Levin et al. 2004). Taken together, the findings are consistent with the clockwise direction of rotation for TM1 during gating (counterclockwise for closure) suggested by site-directed spin-labeling and EPR spectroscopy (Perozo, Cortes et al. 2002).

Interestingly, the data obtained from one mutant in that group (Table 2.1 group II), G30C, seems to not only identify the exposure of the residue without gating, but also indicates that the residue may be buried in the fully open state. *In vivo* data supports this since G30C actually decreases its accessibility upon gating (note the difference between MTSET + shock vs. MTSET-alone values in Table

2.1). When exposed to MTSET from the periplasmic side of the patch, channel gating was altered independent of gating (**Figure 3.3**); G30C gated spontaneously, but rarely achieved fully openings. This could indicate that the residue additional charge inhibits the residue from entering the buried environment within the fully open conformation.

Other residues identified in the SCAM required both exposure to MTSET and osmotic downshock for the largest decrease in viability (Table 2.1 groups IIIa and IIIb) These residues seems to be inaccessible in the closed conformation but become exposed upon channel gating. Previously, modification with MTSET of two of these residues, L19 and G22, yielded decreased open dwell times and gating at lower stimulus (Yoshimura, Batiza et al. 2001; Batiza, Kuo et al. 2002). We observed similar behavior in patch with V23 and I24, also from group III. Interestingly, in patch clamp, channel gating was an absolute requirement for changing the channel activity of V23C (Chapter 3), whereas the *in vivo* experiments suggested some accessibility independent of stimulation by hypo-osmotic treatment (Chapter 2). This slight accessibility is more than likely due to the cytoplasmic membrane having enough tension to gate V23C *in vivo*, since previous studies identified V23C as conferring a strong GOF phenotype when expressed (Levin and Blount 2004). The surprising finding is that I24C was exposed upon gating to MTSET. This residue is tangential to the constriction

point of the closed pore, regardless of whether it is V23 or G26. Exposure of I24 to the pore lumen would require a significant clockwise rotation of TM1, again supporting the Perozo-Martinac model. However, in patch the change in gating properties is observed with the first opening of the channel, unlike the *in vivo* results which predict it to be buried until gating. This discrepancy may be resolved another study which demonstrated the exposure of the I24 residue to the pore prior to ion permeation (Iscla, Levin et al. 2004). Briefly, the study demonstrated that the I24H mutant apparently bound to heavy metals including Ni^{++} and Zn^{++} , which lead to a ‘locking’ into the closed state of the channel. This would occur if the putative clockwise rotation of the TM1 domain occurred prior to ion permeation. Our data would be consistent with this interpretation; although channel activity is not observed in patch while the tension is sub-threshold; one or more of the TM1s may be rotating as a precursor for gating, thereby exposing I24 to a position of accessibility. Together the data strongly suggest that TM1 makes a clockwise rotation to expose I24 during the normal gating process prior to ion permeation, and that the amount of tension in the *in vivo* cytoplasmic membrane is sub-threshold for this motion, yet greater than the threshold for gating of the V23C mutated channel.

The study of G26 has yielded a high informational return from this one residue (its contribution toward the rotation of TM1 is discussed above). The *in*

vivo study revealed a residue exposed to the aqueous vestibule without gating. This is consistent with the proposal that it could be the constriction point in Eco MscL (Iscla, Levin et al. 2004; Levin and Blount 2004). When probed in patch, using MTSET to modify the residue, the channel seems to develop a spontaneous activity and then slowly acquire a 'locked' open state. This finding suggests that more than one MTSET is required to bind to the channel complex before the open-state phenotype is observed. If the G26 residues are truly the constriction point of the channel, then electrostatic interactions may be keeping the channel open. The modified channel seems to prefer a 4/5ths sub-conducting state, perhaps because the fully open state buries the residue within the molecule and steric or energetic constraints inhibit residence in that micro-environment. Finally, G26C was the only residue studied here in patch that showed accessibility, upon gating, to the cytoplasmic side of the channel. G26 remains the most periplasmic residue that is available, upon gating, to the cytoplasmic application of an MTS reagent. Together, these data argue a very unique role and positioning of the G26 residue in the closed, open, and transitional states of the channel.

The second strategy utilized in this study took advantage of the functional differences between homologous MscL channels. Nature itself, in copying *mscL*, has provided sequence variations that still form a mechanosensitive channel. These sequence variations which encode channels with functional differences

may tell us the domains or interactions responsible for channel sensitivity, kinetics, or conductance. The S1/TM1 domains were shown to contribute to the sensitivity and kinetics of the channel in responding to stimuli both *in vivo* and *in vitro*. Furthermore, the TM2/C-terminal domain appears to play a role in setting the shape or size of the open pore.

The N-terminal domain, and specifically TM1, has been implicated in many studies to influencing gating properties of the MscL channel. Random mutagenesis isolated a number of GOF mutants that clustered along one face of TM1 (Ou, Blount et al. 1998). These mutant channels exhibited an increased sensitivity as well as shorter dwell times, often associated with an addition of a more hydrophilic or charged residue. A further study that focused on replacing one particular residue with all of the other available residues found that the hydrophilicity of a residue was important within TM1 (Yoshimura, Batiza et al. 1999), and a hydrophobic gate was postulated to be the main energy barrier in opening MscL (Hamill and Martinac 2001). While short open dwell times of mutant MscL channels have often been correlated with an increased sensitivity that frequently leads to a decrease in cell growth upon induction of channel expression, one does not always predict the other. For instance, *Sau mscL* encodes a channel with very short dwell times (Moe, Blount et al. 1998), but its sensitivity to stimuli is similar to *Eco MscL*. *Tb mscL* encodes a channel with a very low

sensitivity but normal kinetics, compared to Eco MscL (Moe, Levin et al. 2000). Our Eco-Tb chimeras clearly indicate that the S1/TM1 domains play a role in the threshold sensitivity of the channel, but more than a few residues or one domain must be involved because the trait does not cleanly follow any domain.

By making similar S1/TM1 chimeras between Eco and Sau MscL channels, gating kinetics of a channel were also mapped to this region. Out of the 13 S1/TM1 residues that are different between the two sequences, only three seem to be non-conserved substitutions (G22>A, A38>E, and D39>N). A G22A mutation has previously been constructed in *E. coli* MscL, and while the residues are fairly similar, this change has been demonstrated to actually cause the channel to gate less frequently (Yoshimura, Batiza et al. 1999). Considering the other two residues, A38 and D39, it is important to point out that one charge is lost and one is gained, thereby effectively moving the charge one residue over. While A38 has never been isolated in a mutagenic study, we did isolate it in the SCAM assay. The cysteine mutation did not change channel function, but the addition of the charged MTSET at that residue caused a significant growth defect. Since most of the modifications leading to this phenotype are correlated with shorter open dwell times of the channel, it seems possible that this residue plays a role in the effects observed. Given that the mutant is already made and the patch system set up, I think this should be the next cysteine mutant to be characterized.

Moving along the MscL structure, the periplasmic loop is the next domain to fall under examination. Two main studies have been completed that indicate that while the loop does play a role in gating, it is not necessary for the transmission of tension into channel gating. The first study produced MscL as two separate proteins, the N- and C- terminus, within a lipid membrane. The two halves were able to form a mechanosensitive channel, albeit a more sensitive channel (Park, Berrier et al. 2004). In a similar manner, proteases placed on the periplasmic side of the patch caused the channel to gate at a lower threshold, presumably because the periplasmic loop had been eaten away (Ajouz, Berrier et al. 2000). Our data, showing differences between two Eco-Sau chimeras, ES1 and ES2, are consistent with the idea that the loop region plays a role in the elasticity or as an internal ‘spring’ of the channel. Note that ES1, which contains the loop domain from Sau MscL, has open dwell times between and different from both, the Eco and Sau MscL; however inclusion of the Eco MscL loop in ES2 (**Figure 4.3**), generates a channel with kinetics indistinguishable from the Eco MscL. Therefore the periplasmic loop might play a role in open dwell times, possibly by providing ‘stiffness’ to the channel.

By far, one of the most interesting observations in this study, however, is the difference seen in conductions between the Eco and Sau channels and how they map to the TM2/cytoplasmic bundle. A number of orthologues have been

reported to have varying conductances (Moe, Blount et al. 1998; Folgering, Moe et al. 2005), but Sau MscL was not one of them. The open dwell times of the channel are very low, so even though great care was taken in measuring the conductance, it might still be an underestimate. The observation that the TM2/cytoplasmic bundle seems to set the pore size was unexpected, but upon examination not unlikely since TM2 is the domain that interacts directly with the lipids (Chang, Spencer et al. 1998). While we cannot rule out the possibility that the cytoplasmic bundle is responsible for the pore size, much of the cytoplasmic C-terminus has been previously removed and channels were observed with a conductance indistinguishable from Eco MscL (Blount, Sukharev et al. 1996), making it more likely that TM2 alone is responsible for the conductance change. In addition, both the length of the sequence as well as the composition of the cytoplasmic bundle are highly conserved between Eco and Sau MscL. The separately produced N- and C-terminus proteins support this theory because while the N-terminus formed channels, the two portions together were necessary in order to obtain an invariant conductance consistent with wild type MscL (Park, Berrier et al. 2004). One way that TM2 might set the pore size, is by expanding independently of TM1 in order to create a void that the pore lining transmembrane domains can then expand into. Pre-conducting expansion of the channel has been postulated before, but it was theorized that TM1 and TM2 expanded together, leaving the S1 as the final gate (Sukharev, Durell et al. 2001).

From this data, however, it might be proposed that there is only one gate and the movement of TM2 accounts for the pre-expansion. Consistent with this hypothesis, a molecular simulation study by Columbo *et. al.* indicated that TM2 expanded before TM1 during gating in order to create a space for TM1 to occupy (Columbo, Marrink et al. 2003). Regardless, the proposition that TM2 influences the pore size needs to be followed up. Not only by further parsing of the residues responsible for this change in conductance between Eco and Sau MscL, but also by the construction of chimeras between Eco and other homologues with conductance differences such as *B. subtilis* (Moe, Blount et al. 1998).

Some of the questions concerning movement within the channel during gating have been addressed in this study. Residues within the channel pore were identified by using a modified *in vivo* substituted cysteine accessibility method (SCAM; Chapter 2 published as Bartlett, Levin et al. 2004). The SCAM supported the clockwise rotation of TM1 predicted in the PM model and suggested that the closed model of *E. coli* MscL needs to be modified in order to define the fully closed state of the channel. We also examined functional modifications in the pore prior and subsequent to channel activation using the patch clamp technique (Chapter 3) and find unexpected changes in channel kinetics and aqueous availability of some residues. Finally, we gained insight into structural domains that can alter channel threshold tension, kinetics and

conductance by constructing chimeras between Eco and Tb and Eco and Sau
MscLs (Chapter 4).

References

- Operation Manual P-97 Flaming/Brown Micropipette Puller. Novato, CA, Sutter Instrument Company.
- Ajouz, B., C. Berrier, et al. (2000). "Contributions of the different extramembranous domains of the mechanosensitive ion channel MscL to its response to membrane tension." Journal of Biological Chemistry **275**: 1015-22.
- Akabas, M. H. and A. Karlin (1999). Substituted-cysteine accessibility method. Methods in Enzymology, Academic Press. **294**: 123-144.
- Anishkin, A., V. Gendel, et al. (2003). "On the conformation of the COOH-terminal domain of the large mechanosensitive channel MscL." The Journal of general physiology. **121(3)**: 227-44.
- Barron, A., G. May, et al. (1986). "Regulation of envelope protein composition during adaptation to osmotic stress in *Escherichia coli*." J Bacteriol **167(2)**: 433-8.
- Bartlett, J. L., G. Levin, et al. (2004). "An *in vivo* assay identifies changes in residue accessibility on mechanosensitive channel gating." Proc Natl Acad Sci U S A **101**: 10161-10165.
- Bass, R. B., P. Strop, et al. (2002). "Crystal structure of *Escherichia coli* MscS, a voltage-modulated and mechanosensitive channel." Science **298(5598)**: 1582-7.
- Batiza, A. F., M. M. Kuo, et al. (2002). "Gating the bacterial mechanosensitive channel MscL *in vivo*." Proceedings of the National Academy of Sciences of the United States of America **99(8)**: 5643-8.
- Berrier, C., A. Coulombe, et al. (1992). "Gadolinium ion inhibits loss of metabolites induced by osmotic shock and large stretch-activated channels in bacteria." Eur J Biochem **206(2)**: 559-65.
- Betanzos, M., C. S. Chiang, et al. (2002). "A large iris-like expansion of a mechanosensitive channel protein induced by membrane tension." Nature Structural Biology **9(9)**: 704-10.
- Blount, P. (2003). "Molecular mechanisms of mechanosensation: big lessons from small cells." Neuron **37(5)**: 731-4.
- Blount, P. and P. Moe (1999). "Bacterial mechanosensitive channels: integrating physiology, structure and function." Trends in Microbiology **7**: 420-424.
- Blount, P., S. I. Sukharev, et al. (1999). Mechanosensitive channels of bacteria. Methods in Enzymology. P. M. Conn. San Diego, CA, Academic Press. **294**: 458-482.

- Blount, P., S. I. Sukharev, et al. (1996). "Membrane topology and multimeric structure of a mechanosensitive channel protein of *Escherichia coli*." EMBO Journal **15**(18): 4798-805.
- Blount, P., S. I. Sukharev, et al. (1996). "Single residue substitutions that change the gating properties of a mechanosensitive channel in *Escherichia coli*." Proceedings of the National Academy of Sciences of the United States of America **93**(21): 11652-7.
- Booth, I. R. and P. Louis (1999). "Managing hypoosmotic stress: aquaporins and mechanosensitive channels in *Escherichia coli*." Current Opinion in Microbiology **2**(2): 166-9.
- Britten, R. J. and F. T. McClure (1962). "The amino acid pool in *Escherichia coli*." Bacteriol. Rev. **26**: 292-335.
- Cairney, J., I. R. Booth, et al. (1985). "Osmoregulation of gene expression in *Salmonella typhimurium*: proU encodes an osmotically induced betaine transport system." J Bacteriol **164**(3): 1224-32.
- Chang, G., R. H. Spencer, et al. (1998). "Structure of the MscL homolog from *Mycobacterium tuberculosis*: A gated mechanosensitive ion channel." Science **282**: 2220-2226.
- Colombo, G., S. J. Marrink, et al. (2003). "Simulation of MscL gating in a bilayer under stress." Biophys. J. **84**: 2331-2337.
- Corey, D. P., J. Garcia-Anoveros, et al. (2004). "TRPA1 is a candidate for the mechanosensitive transduction channel of vertebrate hair cells." Nature **432**(7018): 723-30.
- Corey, D. P. and C. F. Stevens (1983). Science and technology of patch-recording electrodes. Single-Channel Recording B. S. a. E. Neher. New York, Plenum Press: 53-68.
- Cruickshank, C. C., R. F. Minchin, et al. (1997). "Estimation of the pore size of the large-conductance mechanosensitive ion channel of *Escherichia coli*." Biophysical Journal **73**(4): 1925-31.
- Csonka, L. N. (1988). "Regulation of cytoplasmic proline levels in *Salmonella typhimurium*: effect of osmotic stress on synthesis, degradation, and cellular retention of proline." J Bacteriol **170**(5): 2374-8.
- Csonka, L. N. (1989). "Physiological and genetic responses of bacteria to osmotic stress." Microbiol Rev **53**(1): 121-47.
- Dinnbier, U., E. Limpinsel, et al. (1988). "Transient accumulation of potassium glutamate and its replacement by trehalose during adaptation of growing cells of *Escherichia coli* K-12 to elevated sodium chloride concentrations." Archives of Microbiology **150**(4): 348-57.
- Epstein, W. and S. J. Schultz (1965). "Cation transport in *Escherichia coli*." J. Gen. Physiol. **49**: 221-234.

- Epstein, W., L. Wieczorek, et al. (1984). "Potassium transport in *Escherichia coli*: genetic and biochemical characterization of the K⁺-transporting ATPase." Biochem Soc Trans **12**(2): 235-6.
- Ermakov, Y., A. Averbakh, et al. (2001). "Dipole potentials indicate restructuring of the membrane interface induced by gadolinium and beryllium ions." Biophysical Journal **80**(4): 1851-1862.
- Folgering, J. H., P. C. Moe, et al. (2005). "Lactococcus lactis uses MscL as its principal mechanosensitive channel." J Biol Chem **280**(10): 8784-92.
- Giaever, G. N., L. Snyder, et al. (1988). "DNA supercoiling in vivo." Biophys Chem **29**(1-2): 7-15.
- Gullingsrud, J., K. Schulten, et al. (2003). "Gating of MscL studied by steered molecular dynamics." Biophysical journal. **85**(4): 2087-99.
- Hamill, O. P. and B. Martinac (2001). "Molecular basis of mechanotransduction in living cells." Physiological Reviews **81**(2): 685-740.
- Hamill, O. P. and D. W. McBride (1996). "The pharmacology of mechanogated membrane ion channels." Pharmacological Reviews **48**(2): 231-252.
- Higgins, K. M. and R. S. Lloyd (1987). "Purification of the T4 endonuclease V." Mutat Res **183**(2): 117-21.
- Iscla, I., G. Levin, et al. (2004). "Defining the physical gate of a mechanosensitive channel, MscL, by engineering metal-binding sites." Biophys. J. **87**(5): 3172-80.
- Jones, S. E., R. R. Naik, et al. (2000). "Use of small fluorescent molecules to monitor channel activity." Biochemical & Biophysical Research Communications **279**(1): 208-12.
- Kloda, A. and B. Martinac (2001). "Mechanosensitive channels in archaea." Cell Biochemistry & Biophysics **34**(3): 349-81.
- Laimins, L. A., D. B. Rhoads, et al. (1981). "Osmotic control of kdp operon expression in *Escherichia coli*." Proceedings of the National Academy of Sciences of the United States of America **78**(1): 464-8.
- Lee, A. G. (1998). "How lipids interact with an intrinsic membrane protein: the case of the calcium pump." Biochim Biophys Acta **1376**(3): 381-90.
- Levin, G. and P. Blount (2004). "Cysteine scanning of MscL transmembrane domains reveals residues critical for mechanosensitive channel gating." Biophys J **86**(5): 2862-70.
- Levina, N., S. Totemeyer, et al. (1999). "Protection of *Escherichia coli* cells against extreme turgor by activation of MscS and MscL mechanosensitive channels: identification of genes required for MscS activity." EMBO Journal **18**(7): 1730-1737.
- Li, Y., P. C. Moe, et al. (2002). "Ionic regulation of MscK, a mechanosensitive channel from *Escherichia coli*." EMBO J. **21**(20): 5323-5330.

- Lindahl, E. and O. Edholm (2000). "Mesoscopic undulations and thickness fluctuations in lipid bilayers from molecular dynamics simulations." Biophys J **79**(1): 426-33.
- Maingret, F., A. Patel, et al. (2000). "Lysophospholipids open the two-pore domain mechano-gated K(+) channels TREK-1 and TRAAK." Journal of Biological Chemistry **275**: 10128-10133.
- Martinac, B., J. Adler, et al. (1990). "Mechanosensitive ion channels of *E. coli* activated by amphipaths." Nature **348**(6298): 261-263.
- Martinac, B., M. Buechner, et al. (1987). "Pressure-sensitive ion channel in *Escherichia coli*." Proceedings of the National Academy of Sciences of the United States of America **84**(8): 2297-301.
- Maurer, J. A. and D. A. Dougherty (2001). "A high-throughput screen for MscL channel activity and mutational phenotyping." Biochimica et Biophysica Acta **1514**(2): 165-9.
- Maurer, J. A. and D. A. Dougherty (2003). "Generation and evaluation of a large mutational library from the *Escherichia coli* mechanosensitive channel of large conductance, MscL - Implications for channel gating and evolutionary design." Journal of Biological Chemistry **278**(23): 21076-21082.
- Measures, J. C. (1975). "Role of amino acids in osmoregulation of non-halophilic bacteria." Nature **257**(5525): 398-400.
- Moe, P. and P. Blount (2005). "Assessment of potential stimuli for mechano-dependent gating of MscL: effects of pressure, tension, and lipid headgroups." Biochemistry **44**(36): 12239-44.
- Moe, P. C. and P. Blount (2002). A novel approach for probing protein-lipid interactions of MscL, a membrane-tension-gated channel. Biophysical chemistry: membranes and proteins. R. H. Templer and R. Leatherbarrow, Royal Society of Chemistry (UK): 199-207.
- Moe, P. C., P. Blount, et al. (1998). "Functional and structural conservation in the mechanosensitive channel MscL implicates elements crucial for mechanosensation." Molecular Microbiology **28**: 583-592.
- Moe, P. C., G. Levin, et al. (2000). "Correlating a protein structure with function of a bacterial mechanosensitive channel." Journal of Biological Chemistry **275**(40): 31121-7.
- Nakamaru, Y., Y. Takahashi, et al. (1999). "Mechanosensitive channel functions to alleviate the cell lysis of marine bacterium, *Vibrio alginolyticus*, by osmotic downshock." FEBS Letters **444**(2-3): 170-172.
- Nazarenko, L. V., I. M. Andreev, et al. (2003). "Calcium release from *Synechocystis* cells induced by depolarization of the plasma membrane: MscL as an outward Ca²⁺ channel." Microbiology **149**(Pt 5): 1147-53.

- Ou, X., P. Blount, et al. (1998). "One face of a transmembrane helix is crucial in mechanosensitive channel gating." Proceedings of the National Academy of Sciences of the United States of America **95**(19): 11471-5.
- Park, K. H., C. Berrier, et al. (2004). "Purification and functional reconstitution of N- and C-halves of the MscL channel." Biophysical Journal **86**(4): 2129-2136.
- Perozo, E., D. M. Cortes, et al. (2002). "Open channel structure of MscL and the gating mechanism of mechanosensitive channels." Nature **418**(6901): 942-8.
- Perozo, E., A. Kloda, et al. (2001). "Site-directed spin-labeling analysis of reconstituted MscL in the closed state." Journal of General Physiology **118**(2): 193-206.
- Perozo, E., A. Kloda, et al. (2002). "Physical principles underlying the transduction of bilayer deformation forces during mechanosensitive channel gating." Nature Structural Biology **9**(9): 696-703.
- Pivetti, C. D., M. R. Yen, et al. (2003). "Two families of mechanosensitive channel proteins." Microbiology and Molecular Biology Reviews **67**(1): 66-85.
- Powl, A. M., J. N. Wright, et al. (2005). "Identification of the Hydrophobic Thickness of a Membrane Protein Using Fluorescence Spectroscopy: Studies with the Mechanosensitive Channel MscL(,)(1)." Biochemistry **44**(15): 5713-21.
- Rhoads, D. B. and W. Epstein (1978). "Cation transport in Escherichia coli. IX. Regulation of K transport." Journal of General Physiology **72**(3): 283-95.
- Sukharev, S., M. Betanzos, et al. (2001). "The gating mechanism of the large mechanosensitive channel MscL." Nature **409**(6821): 720-724.
- Sukharev, S. and D. P. Corey (2004). "Mechanosensitive channels: multiplicity of families and gating paradigms." Sci STKE **2004**(219): re4.
- Sukharev, S., S. Durell, et al. (2001). "Structural models of the MscL gating mechanism." Biophys. J. **81**(2): 917-936.
- Sukharev, S. I., P. Blount, et al. (1994). "A large-conductance mechanosensitive channel in *E. coli* encoded by *mscL* alone." Nature **368**(6468): 265-8.
- Sukharev, S. I., B. Martinac, et al. (1994). "Functional reconstitution as an assay for biochemical isolation of channel proteins: Application to the molecular identification of a bacterial mechanosensitive channel." Methods: A Companion to Methods in Enzymology **6**(1): 51-9.
- Sukharev, S. I., M. J. Schroeder, et al. (1999). "Stoichiometry of the large conductance bacterial mechanosensitive channel of *E. coli*. A biochemical study." Journal of Membrane Biology **171**(3): 183-93.

- Tavernarakis, N. and M. Driscoll (1997). "Molecular modeling of mechanotransduction in the nematode *Caenorhabditis elegans*." Annual Review of Physiology **59**: 659-689.
- Yoshimura, K., A. Batiza, et al. (2001). "Chemically charging the pore constriction opens the mechanosensitive channel MscL." Biophysical Journal **80**(5): 2198-2206.
- Yoshimura, K., A. Batiza, et al. (1999). "Hydrophilicity of a single residue within MscL correlates with increased channel mechanosensitivity." Biophysical Journal **77**: 1960-1972.

VITAE

Jessica Louise Bartlett was born in Marietta, Georgia, on October 2, 1976, the daughter of Cheryl McFarlane Bartlett and Donald Lewis Bartlett. After completing her work at Lassiter High School, Marietta, Georgia in 1995, she entered Auburn University at Auburn, Alabama. She received the degree of Bachelor of Science with a major in biochemistry from Auburn University in March, 2000. In September, 2000 she entered the Graduate School of Biomedical Sciences at the University of Texas Southwestern Medical Center at Dallas. She was awarded the degree of Doctorate of Philosophy in June, 2006.

Permanent Address: 719 Jamie Way
Woodstock, Georgia 30188